NASA Contractor Report 185134

# Conceptual Design Study of a 5 Kilowatt Solar Dynamic Brayton Power System Using a Dome Fresnel Lens Solar Concentrator

Mark J. O'Neill, A.J. McDanal and Don H. Spears

*ENTECH, Inc.*

*Dallas-Fort Worth Airport, Texas*

December 1989

Prepared for
Lewis Research Center
Under Contract NAS3-24877

National Aeronautics and
Space Administration

# CONCEPTUAL DESIGN STUDY OF A 5 KILOWATT SOLAR DYNAMIC BRAYTON POWER SYSTEM USING A DOME FRESNEL LENS SOLAR CONCENTRATOR

(Final Technical Report for NASA Lewis Research Center Contract No. NAS3-24877)

## Contents

# 1.0 SUMMARY

The primary objective of this project was to generate a conceptual design for a nominal 5 kW (electric) solar dynamic space power system, which uses a unique, patented, transmittance-optimized, dome-shaped, point-focus Fresnel lens as the optical concentrator element. Compared to more conventional reflective concentrators, the dome Fresnel lens allows 200 times larger slope errors for the same image displacement. Such larger allowable shape errors translate into higher allowable deflections and correspondingly lighter concentrator designs. Additionally, the dome Fresnel lens allows the energy receiver, the power conversion unit (PCU), and the heat rejection radiator to be independently optimized in configuration and orientation, since none of these elements causes any aperture blockage. In contrast, reflective concentrators often require compromises in the designs of these elements to minimize their aperture shading effects. Since the dome Fresnel lens is comprised of literally thousands of individual prisms, this approach offers a better opportunity than reflective approaches for tailoring the radiant flux distribution within the receiver, by slightly altering the design of these microscopic prisms.

The conceptual design is based on NASA-furnished parameters regarding the orbit (Low Earth Orbit [LEO]), the receiver temperature (1121 K), the Brayton cycle PCU efficiency (23.7%), the sun-tracking error (0.25 degree), and the required system electrical output (5 kW). Based on optical and thermal analyses, a recommended conceptual design has been developed for the new concentrator, which provides an aperture diameter of 6.6 meters, has an optical axis focal length of 7.2 meters, and is optimized to focus into a cavity receiver with an entrance aperture diameter of 0.23 meters. Expected lens net optical efficiency is about 87% without antireflection coatings, and higher with such coatings. The recommended system is designed to provide 5 kW of continuous electrical power throughout a 93 minute LEO orbital period, including 36 minutes of eclipse. Excess heat is collected and stored in the receiver during the illuminated portion of the orbit, to provide needed energy during the eclipse portion of the orbit.

Optical analyses and thermal analyses led to the selection of a 30 degree rim angle and an 800X geometric concentration ratio for the dome lens. An approach for subdividing the large dome lens into manageable gores, panels, and parquet elements was developed. A relatively simple approach to gore stowage and automatic deployment was generated. Finite element structural analyses were performed to size graphite/epoxy lens support structure elements to withstand 1.5 G loading. The resultant structure has a natural frequency of 0.5 Hertz. The total mass of lens panels (assuming microglass construction), support structure (graphite/epoxy composite), and miscellaneous hardware is estimated to be about 1.2 kilograms per square meter of aperture.

The key problem area for the dome lens approach has related to lens material selection. Numerous moldable polymers, with and without various coatings, have been evaluated, but all have suffered optical performance degradation under simulated LEO atomic oxygen exposure in the NASA Lewis "asher" test facility. Only glass has survived such tests without performance degradation. Under the present NASA-supported program, all-glass Fresnel lens samples were successfully made for the first time by a "sol-gel" casting process. While much further process development work is needed to establish the practicality of manufacturing thin, large-area lens panels, the technical feasibility of making high-quality, sol-gel glass Fresnel lenses has now been demonstrated.

## 2.0 INTRODUCTION

For many years, NASA has conducted research and development activities related to solar dynamic space power systems (Reference 1). Such a solar dynamic system uses an optical concentrator to focus sunlight into a high-temperature heat receiver, which provides the thermal energy for a power converion unit (PCU), which is based on a thermodynamic heat engine cycle. In the middle 1980's, NASA's interest in solar dynamic space power systems intensified, as the potential advantages of such systems for application to the Space Station became quantified (Reference 2). With current Brayton cycle heat engine technology, a thermal-to-electrical conversion efficiency of about 24% should be achievable under orbital operation (Reference 3). With a high-quality, point-focus solar concentrator, a solar-to-thermal conversion efficiency of about 75% should be achievable under orbital conditions (Reference 4). Thus, the overall solar-to-electrical conversion efficiency should be about 18% for a properly designed solar dynamic power system. Furthermore, thermal energy storage can be efficiently integrated into the heat receiver to provide needed energy for the eclipse portion of an orbit. Compared to state-of-the-art silicon photovoltaic arrays, coupled with electrical energy storage for the eclipse portion of an orbit, the solar dynamic system clearly offers a much higher overall conversion efficiency and a simpler approach to energy storage (Reference 5).

The most basic element in a solar dynamic space power system is the energy-collecting optical concentrator. While there are many approaches to solar concentrators, the most conventional approach for a solar dynamic space power system has been the reflective parabolic dish solar concentrator. However, the parabolic dish has several significant disadvantages for space power applications, as described in the following paragraphs.

The energy receiver, the PCU, and the waste heat rejection radiator must all be located at or near the focal point of the parabolic dish to function efficiently. In such a location, these elements and their supporting structures generally shade the dish aperture, thereby reducing solar energy collection efficiency. To minimize such shading, design compromises are required. Dish shading can be eliminated by using an offset (non-axisymmetric) parabola (Reference 6). However, this offset parabola approach increases image size and decreases image uniformity, thereby reducing receiver thermal efficiency. To minimize radiator shading, the radiator can be oriented parallel to the solar rays, i.e., edge-facing-sun. However, the optimal radiator orientation is edge-facing-earth to minimize albedo and infrared irradiance, and edge-facing-forward to minimize aerodynamic drag due to residual atmospheric gasses. Clearly, the edge-facing-sun restraint requires either the desired thermal or the desired aerodynamic orientation to be sacrificed. Similarly, structural members which support the receiver, PCU, and radiator must be designed to minimize aperture shading, rather than being optimized from stiffness/mass considerations.

In addition to shading problems, parabolic dish solar concentrators require precise shape maintenance for good focussing performance. Such precise control of dish shape has proven to be exceptionally difficult even for relatively heavy terrestrial concentrators under varying operating conditions (Reference 7). For orbital operation, with the inevitable large temperature variations associated with the illuminated versus eclipsed periods of the orbit, shape control will be even more difficult for the ultra-light space concentrators needed for solar dynamic power systems.

Another problem area for parabolic dish concentrators relates to the radiant flux distribution produced near the focal point (Reference 8). Most dishes produce very high spikes of irradiance at the center of the solar image, which can cause receiver heat transfer problems during normal operation, and safety problems during periods of abnormal sun-tracking. Also, the flux distribution over active heat transfer surfaces within the receiver will vary with the local shape errors of the corresponding regions of the dish which are illuminating that portion of the receiver.

To overcome some of these shortcomings of conventional parabolic dish solar concentrators, refractive optical systems can be used in place of reflective optical systems (Reference 9). Refractive systems eliminate all of the receiver, PCU, and radiator shading problems, since these elements are naturally located behind the lens. Therefore, the receiver and PCU designs can be optimized from heat transfer and thermodynamic considerations; the radiator orientation can be optimized from thermal and aerodynamic considerations; and the structures which support the receiver, PCU, and radiator can be optimized from stiffness/mass considerations. Thus, refractive systems offer significant advantages over reflective systems relative to aperture shading.

To overcome problems associated with precise shape maintenance, a unique type of refractive concentrator must be used (Reference 10). When a dome-shaped Fresnel lens is configured such that each prism within the lens has essentially equal angles of incidence and emergence for rays of sunlight transmitted through that prism, the lens provides a remarkable tolerance for slope errors which is two full orders of magnitude larger than for a reflective concentrator (Reference 11). Due to the symmetrical refraction condition imposed on each prism, the dome lens can tolerate slope errors which are 200 times as large as those in a parabolic dish, with equal image displacement. Furthermore, the symmetrical refraction condition minimizes reflection losses and thereby maximizes lens transmittance.

To overcome radiant flux distribution problems, the dome Fresnel lens concentrator provides excellent potential for flux profile tailoring. Since the dome lens consists of many thousands of individual prisms, the angles of these prisms can be slightly altered in design to provide the desired radiant flux distribution (Reference 12). Such flux profile tailoring results in milder irradiance spikes at the center of the solar image, and gentler, more uniform irradiance profiles over receiver heat transfer surfaces.

In 1985, NASA Lewis Research Center selected Harris Corporation as the prime contractor for the Solar Concentrator Advanced Development (SCAD) Program (Reference 13). Under this program, Harris and its subcontractors (including ENTECH) evaluated several parabolic dish concepts and the dome Fresnel lens concept. Conceptual designs of nominal 25 kW (electric) concentrators were developed for the various concentrator candidates, to allow comparisons regarding area, mass, stow volume, deployability, and other considerations. The recommended design concept from the Harris comparison was an offset parabolic dish with interlocking hexagonal reflective elements. However, compared to the selected parabolic dish concept, the dome lens concept was found by Harris to offer significantly lower mass, greatly reduced stow volume, automatic deployment instead of astronaut-assisted assembly, and very competitive predicted performance. Unfortunately, the lens material issue was the Achilles' heel for

the dome lens concept in this early Harris evaluation. All of the candidate lens materials empirically evaluated during the Harris study suffered optical performance degradation due to atomic oxygen erosion in "asher" testing at NASA Lewis. The rapid hardware development schedule planned for the SCAD project precluded the selection of the dome lens approach, due to the risks associated with the unresolved lens material issue.

In 1986, NASA Lewis inititated the program documented in this final technical report. The primary objective of this program was to develop a conceptual design for a more optimized and smaller scale dome Fresnel lens space solar dynamic concentrator. In particular, the new design was to utilize a 5 kW (electric) Brayton cycle power conversion unit (PCU) and was to be deployed in low earth orbit (LEO). Based on NASA-furnished design parameters, and on optical and thermal trade studies, a conceptual design has been generated. The recommended dome lens concentrator concept offers excellent performance, low mass, compact stowage, and a straightforward approach to automatic deployment. In addition, an exciting new lens material approach, which should offer excellent durability in the orbital environment, has been identified. The new lens material is densified "sol-gel" glass. Small "sol-gel" prismatic lens samples were successfully made and evaluated under this program.

The following sections of this report describe the dome lens concept, summarize the recommended 5 kW (electric) concentrator approach, present results of optical, thermal, and structural analyses, provide concentrator performance and mass estimates, and discuss lens material evaluations. The key conclusion drawn from this study is that the dome lens concentrator approach offers a number of significant advantages over conventional parabolic dish approaches for space solar dynamic power system applications.

## 3.0 DESCRIPTION AND ADVANTAGES OF THE DOME FRESNEL LENS

Figure 3-1 shows an artist's concept of a large-area, point-focus, dome Fresnel lens concentrator for space solar dynamic power applications. The design depicted in this figure was developed in 1985-86 by Harris Corporation and ENTECH, Inc., under the NASA Lewis-funded Solar Concentrator Advanced Development (SCAD) project. This concentrator is sized at about 15 meters in aperture diameter, corresponding to a nominal 25 kW (electric) solar dynamic power module. This design utilizes the Harris Deployable Radial Truss Structure (DRTS) system for automatic deployment and lens/receiver support on orbit. Under the present program, a conceptual design has been generated for a smaller version of the dome Fresnel lens space solar dynamic concentrator, sized for a 5 kW (electric) Brayton cycle power module.

Regardless of concentrator size, the dome lens solar concentrator uses a unique optical design. Figure 3-2 shows a highly magnified cross sectional view of a small portion of the dome lens. The convex outer lens surface is smooth, while the concave inner lens surface is faceted with microscopic prisms. Each prism is typically 100 to 200 micrometers in height, with a configuration different from every other prism in the lens. As shown in Figure 3-2, for each individual prism, the angle of incidence of the solar rays at the smooth outer lens surface is equal to the angle of emergence of the solar rays at the inner faceted lens surface. This symmetrical refraction condition provides a multitude of optical performance benefits, compared to other Fresnel lens designs. As thoroughly discussed in previous publications (References 10 through 12), the symmetrical refraction condition provides the lowest possible reflection losses for each prism, thereby maximizing the transmittance of the entire lens. The unusual curved shape of the transmittance-optimized dome lens is uniquely defined by the symmetrical refraction constraint (Reference 10).

In addition to transmittance advantages, each symmetrical refraction prism provides a much smaller solar image than alternate non-symmetrical refraction prisms with the same total ray turning angle, when the combined effects of finite solar disk size, chromatic aberration, prism manufacturing inaccuracies, and prism orientation inaccuracies are considered (Reference 11). Since prism orientation inaccuracies correspond directly to concentrator slope errors, image defocussing due to this inaccuracy is extremely important. Compared to conventional flat Fresnel lenses, the symmetrical refraction lens allows 100 times larger slope errors for equal image defocussing (Reference 11). Compared to reflective solar concentrators, the symmetrical refraction lens allows 200 times larger slope errors for equal image defocussing (Reference 11). Figure 3-3 shows the relative image displacement for a parabolic dish and the symmetrical refraction dome lens due to a $\pm$ 1 degree slope error, for equal concentrator size and rim angle, at the same ray location relative to the optical axis. The total image displacement is nearly 55 cm for the dish, and only 0.14 cm for the lens.

This unequaled tolerance for slope errors is due to the symmetry of refraction for the dome lens. If a slope error causes the ray incidence angle (Figure 3-2) to increase by 1 degree (for example), then the ray emergence angle will be reduced by the same 1 degree, resulting in the total ray turning angle remaining unchanged. No other type of concentrator offers this tremendous slope error tolerance. This tolerance of slope errors means that the dome lens shape is not critical to good optical performance. Therefore, the accuracies required for concentrator manufacture and deployment can be relaxed, and allowable structural

ENTECH, INC.

Figure 3-1

BACKGROUND:
NASA DOME LENS BRAYTON PROGRAM
HARRIS CORPORATION SCAD DESIGN
OF ENTECH DOME LENS CONCENTRATOR

## DOMED FRESNEL CONCENTRATOR

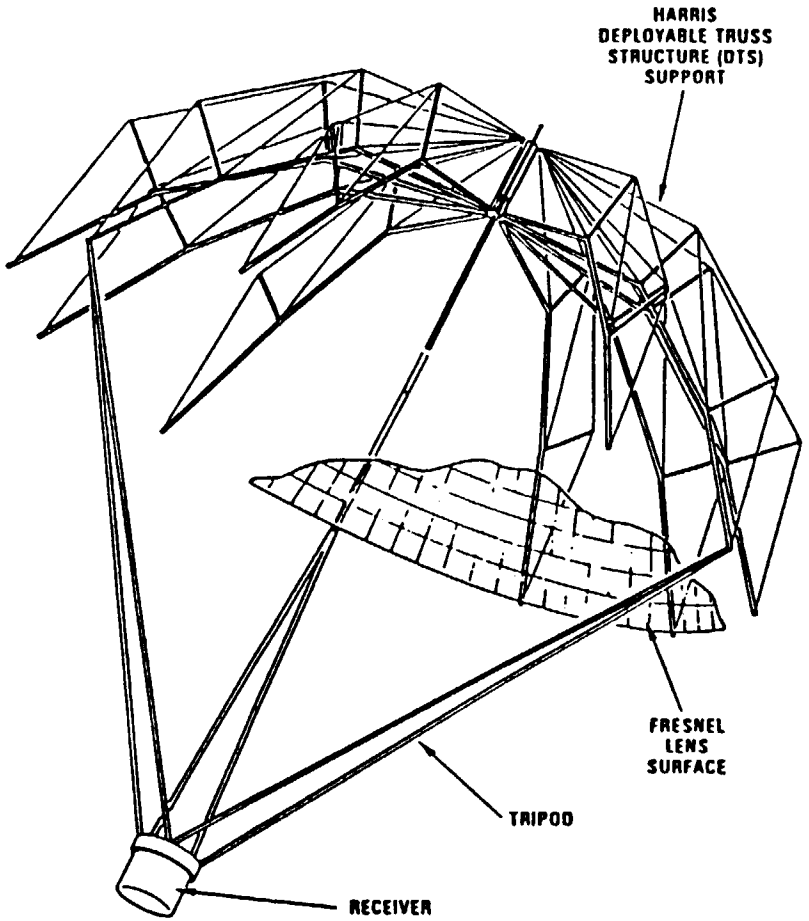

Figure 3-2
MAGNIFIED VIEW OF PRISMS WITHIN ENTECH LENS, SHOWING SYMMETRIC REFRACTION AND BLUNT TIP TOLERANCE

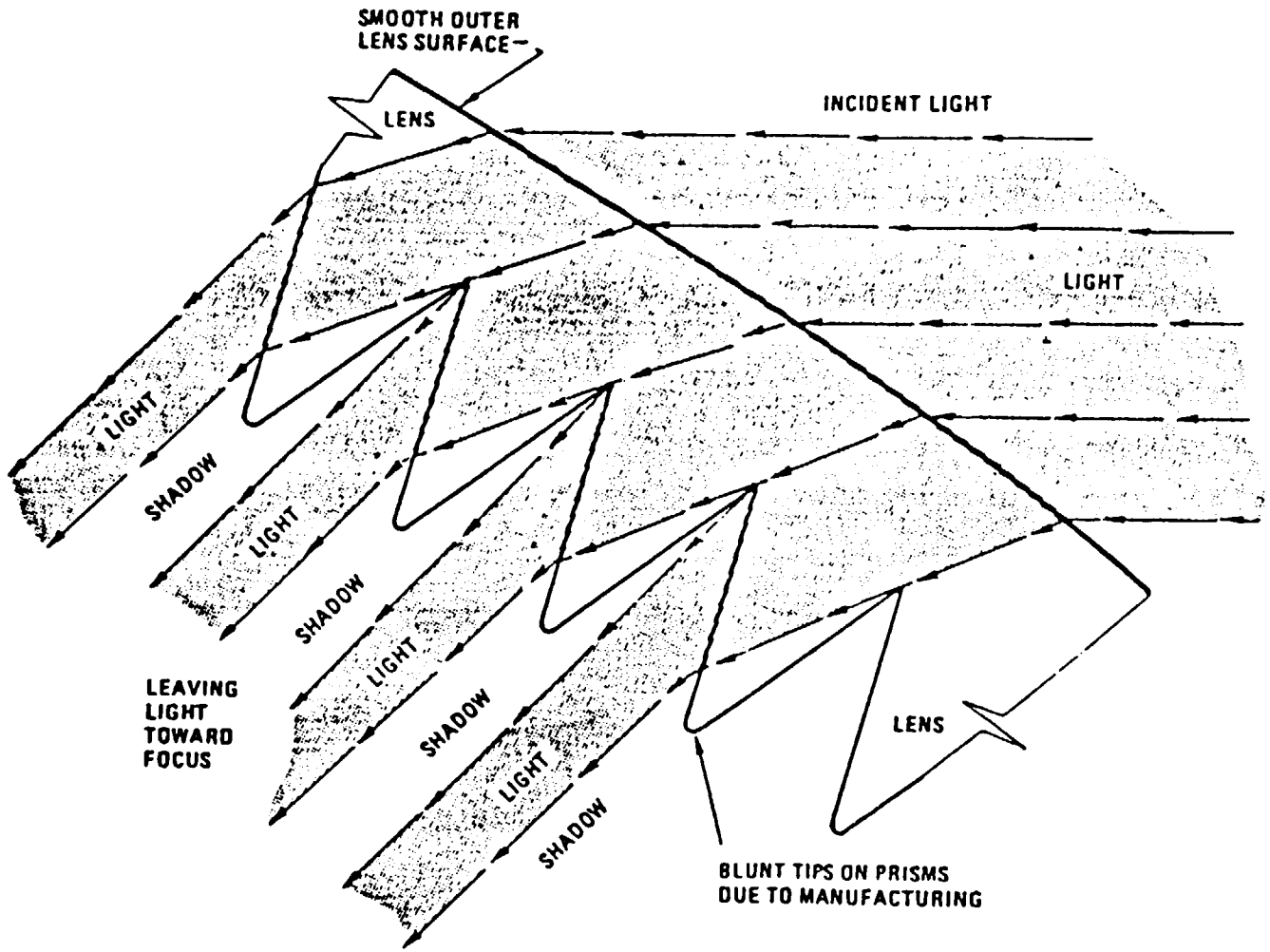

ENTECH, INC.

Figure 3-3
SLOPE ERROR EFFECT ON REFLECTIVE CONCENTRATOR VERSUS DOME LENS CONCENTRATOR
(55 cm VERSUS 0.28 cm DEFOCUS DIAMETER)

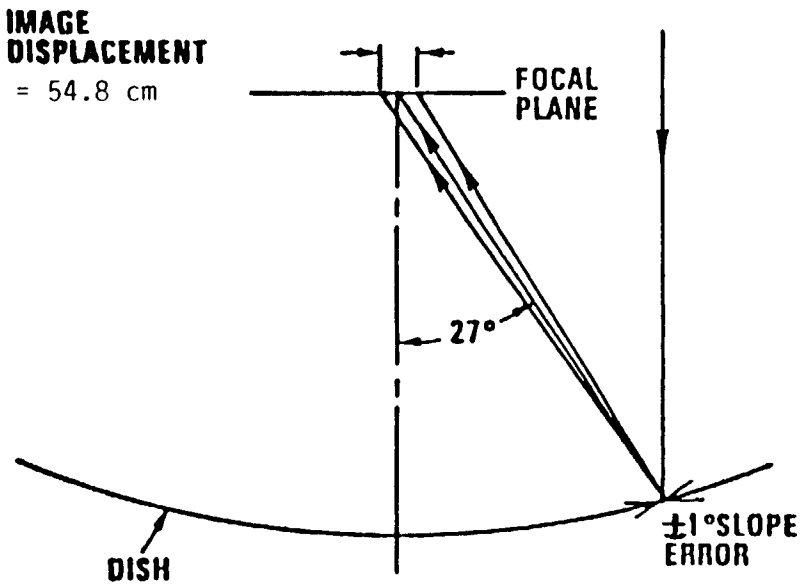


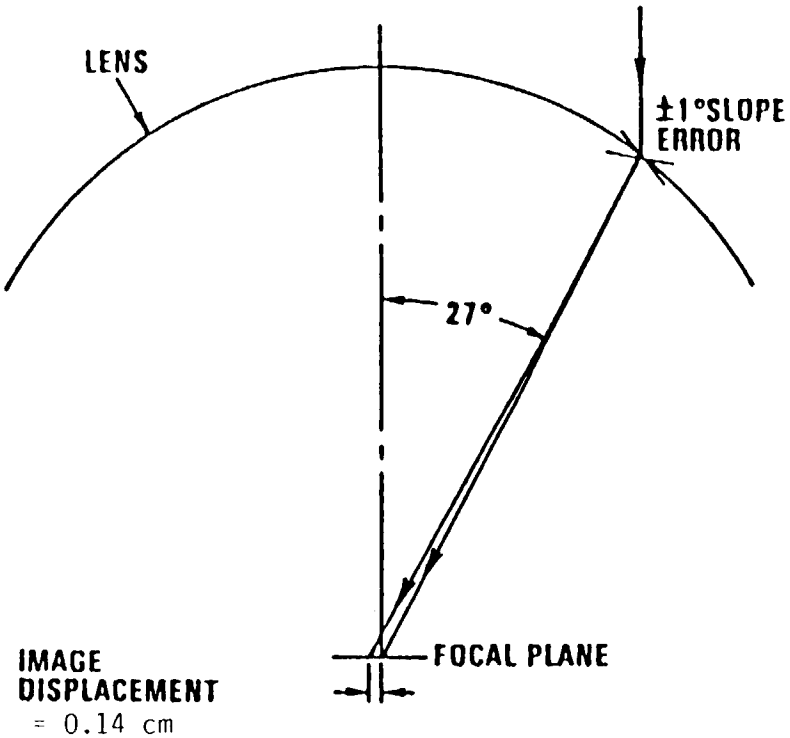


**PARABOLIC DISH**

- 45° RIM ANGLE
- 11 METER APERTURE
- ±1° SLOPE ERROR AT 27° LOCAL RIM ANGLE
- PLUS AND MINUS SLOPE ERRORS CAUSE EQUAL DISPLACEMENTS IN OPPOSITE DIRECTIONS

**FRESNEL LENS**

- 45° RIM ANGLE
- 11 METER APERTURE
- ±1° SLOPE ERROR AT 27° LOCAL RIM ANGLE
- PLUS AND MINUS SLOPE ERRORS CAUSE EQUAL DISPLACEMENTS IN SAME DIRECTION

deflections can be increased. Thus, the slope error tolerance relates directly to lower concentrator mass.

Referring back to Figure 3-1, another major advantage of the dome lens approach over reflective parabolic dish concentrators becomes apparent. The thermal energy receiver, the power conversion unit (PCU), the waste heat dissipation radiator, and the supporting structures for these elements (not all shown in the figure) are all located behind the lens and therefore out of the path of the sunlight. In contrast, for a parabolic dish system, all of these elements are between the sun and the dish, thereby causing significant aperture shading and blockage losses.

Another significant advantage of the dome lens approach relates to radiant flux profile tailoring. Since the lens consists of literally thousands of microscopic prisms (Figure 3-2), the individual solar image produced by each prism can be directed to any desired location in the focal region, by selecting the prism apex angle accordingly. Since the final focal region irradiance distribution is simply the integral of the contributions from all of the prisms in the lens, the lens design has several thousand degrees of freedom (one for each prism in the lens) to tailor this irradiance profile. This flux profile tailoring has been successfully accomplished for several different versions of terrestrial solar concentrator lenses of the same basic optical design for more than a decade (Reference 12). By properly selecting the dome lens prisms for the space solar dynamic concentrator application, a mild irradiance profile over the heat absorption surfaces within the thermal receiver can be designed to match the heat transfer requirements of the receiver. In addition, the irradiance profile can be designed to avoid tremendous flux spikes at the center of the focus, which are common with parabolic dish concentrators, and which can and do cause safety problems when the sun-tracking system malfunctions for any reason (Reference 8).

In summary, the dome lens approach offers substantial advantages over the reflective parabolic dish approach for solar dynamic power system applications. However, an optimal material for the lens must be identified and proven. The ideal material would be highly transparent over the full solar spectrum (0.3 to 2.5 micrometers), easy to mold into the desired prismatic geometry, light weight, durable under low earth orbit (LEO) exposure (including ultraviolet radiation, particulate radiation, atomic oxygen, widely variable temperature, micro-meteoroids, etc.), and relatively low cost. Unfortunately, such an ideal lens material remains to be found, as further discussed in Section 9.0. Several different polymer material candidates have been evaluated, but protective coatings must be developed to protect these materials from atomic oxygen in particular, as discussed in Section 9.1. In addition to these polymers, another candidate material (sol-gel glass) has been identified and shown to be moldable into the required prismatic geometry, as discussed in Section 9.2. This glass material should offer excellent durability in the orbital environment.

The following section presents the NASA-furnished design parameters which were used to generate the conceptual design of a nominal 5 kW (electric) Brayton cycle dome Fresnel lens solar dynamic space concentrator.

## 4.0 NASA-FURNISHED DESIGN PARAMETERS

At the beginning of this conceptual design study, NASA Lewis furnished several parameters to be used in the analysis and optimization of the dome Fresnel lens solar dynamic space concentrator. Figure 4-1 summarizes these parameters. A low earth orbit (LEO) altitude of 500 kilometers was specified, to be compatible with the operating capabilities of both the existing NASA Space Transportation System (Space Shuttle) and the planned NASA Space Station. This orbit corresponds to a 93 minute period, including 57 minutes of solar illumination and 36 minutes of eclipse.

The power conversion unit (PCU) specified by NASA Lewis is a 5 kW (electric) Brayton cycle heat engine coupled to an alternator. The overall conversion efficiency of the PCU, including power management and distribution losses, is 23.7%. Including a small temperature increase for thermal storage to be integrated within the receiver, such that heat will be available to the PCU during the eclipse portion of the orbit, NASA Lewis estimated the receiver temperature at 1121 K. For radiation heat loss calculations, NASA specified a heat sink temperature of 225 K.

For optical calculations, NASA specified a maximal value for the sun-tracking error of 0.25 degrees.

For power and energy calculations, which relate directly to lens aperture requirements, NASA specified a 5 kW (electric) continuous system power output. This power level corresponds to 27900 kJ of electrical energy production per orbit.

These NASA-furnished parameters were used to size the dome lens during optical and thermal trade studies. After numerous iterations, the concentrator system described briefly in the following section was recommended.

Figure 4-1
NASA-FURNISHED DESIGN PARAMETERS

**ORBIT:** 500 KILOMETER ALTITUDE
93 MINUTES TOTAL PERIOD
57 MINUTES ILLUMINATED
36 MINUTES ECLIPSED

**THERMAL:**
RECEIVER TEMP. = 1121 K
RADIATION SINK TEMP. = 225 K

**POWER CONVERSION UNIT:**

| | |
|---|---|
| BRAYTON ENGINE EFFICIENCY | = 0.293 |
| ALTERNATOR EFFICIENCY | = 0.900 |
| POWER MGT & DIST EFFICIENCY | = 0.900 |
| OVERALL PCU EFFICIENCY | = 0.237 |

**DESIGN TRACKING ERROR:** ±0.25 DEGREES MAX

**SYSTEM OUTPUT:** 5 kW CONTINUOUS ELECTRICAL POWER
27,900 kJ PER ORBIT

## 5.0 SUMMARY OF THE RECOMMENDED DESIGN

Based on the NASA-furnished design parameters presented in the previous section, and the results of optical and thermal analyses discussed in the following sections, the 5 kW (electric) dome lens solar dynamic concentrator system summarized in Figure 5-1 represents the recommended system design. The gross aperture diameter is 6.61 meters, for a total aperture area of 34.3 sq.m. With a structural blockage of about 5%, the net aperture area is 32.6 sq.m. As discussed in Section 6.0, the expected lens optical efficiency is 86.7%. The product of lens efficiency, net aperture area, and the orbital solar constant of 1.353 kW/sq.m. corresponds to a receiver thermal power input of 38.2 kW (thermal). During the illuminated portion of the orbit, 130.7 MJ of heat energy will be input to the receiver.

The receiver is assumed to be an insulated cavity with an aperture opening of 0.234 m in diameter, for a total aperture area of 0.0429 sq.m. Black-body radiation losses from this receiver aperture area are 3.8 kW (thermal). Assuming that the receiver aperture is automatically covered with an insulated lid during the eclipse portion of the orbit, total radiation loss per orbit is 13.0 MJ. Subtracting the receiver heat loss per orbit from the receiver input heat rate per orbit results in a net receiver heat gain of 117.7 MJ per orbit.

With the overall PCU heat to electricity conversion efficiency of 23.7%, including thermodynamic cycle, alternator, and power management and distribution (PMAD) efficiencies, 21.1 kW (thermal) is required as the heat input to the PCU to produce 5 kW (electric). To provide 5 kW (electric) continuously over the full orbit, the required heat input to the PCU is 117.7 MJ, matching the net receiver heat gain of the previous paragraph.

The following sections describe the optical and thermal trade studies that led to the recommended design presented above.

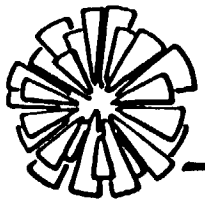

ENTECH, INC.

Figure 5-1

RECOMMENDED 5 $KW_e$ DOME LENS/BRAYTON SOLAR DYNAMIC POWER SYSTEM

## SIZING & ENERGY BALANCE

| | | | |
|---|---|---|---|
| 1. | Gross Aperture Diameter | 6.61 m | 21.7 ft |
| 2. | Gross Aperture Area | 34.3 sq.m. | 369 sq.ft. |
| 3. | Structural Blockage Factor | 0.95 | |
| 4. | Net Aperture Area | 32.6 sq.m. | 351 sq.ft. |
| 5. | Optical Efficiency (800X) | 0.867 | |
| 6. | Receiver Input Heat Rate | 38.2 kW | 131 kBTU/hr |
| 7. | Receiver Orbital Heat Input (57 min) | 130.7 MJ | 124 kBTU |
| 8. | Receiver Aperture Diameter | 0.234 m | 0.767 ft |
| 9. | Receiver Aperture Area | 0.0429 sq.m. | 0.462 sq.ft. |
| 10. | Receiver Heat Loss Rate (1121K to 225K) | 3.8 kW | 13 kBTU/hr |
| 11. | Receiver Orbital Heat Loss (57 min) (Closed Cavity during Eclipse) | 13.0 MJ | 12 kBTU |
| 12. | Receiver Orbital Net Heat Gain (57 min) | 117.7 MJ | 112 kBTU |
| 13. | Brayton Engine Efficiency (NASA-Supplied) | 0.293 | |
| 14. | Alternator Efficiency (NASA-Supplied) | 0.90 | |
| 15. | Power Mgmt & Dist Effy (NASA-Supplied) | 0.90 | |
| 16. | Engine Heat Rate Requirement (for 5 $kW_e$) | 21.1 kW | 72 kBTU/hr |
| 17. | Engine Orbital Heat Requirement (93 min) (Balances with Item 12 above) | 117.7 MJ | 112 kBTU |

## 6.0 OPTICAL ANALYSIS AND DISCUSSION

Over the past dozen years, ENTECH has developed, refined, and empirically verified sophisticated computer programs for analyzing, optimizing, and designing Fresnel lens solar concentrators (e.g., Reference 12). These programs are based on dispersive cone optics methods, under which rays from various portions of the solar disk, of various wavelengths over the solar spectrum, intercept various regions of the lens aperture, from which the rays are analytically traced through the lens, with proper accounting for reflection and absorption losses, until the rays finally intercept the focal plane and the energy receiver surfaces. A numerical integration of all such rays provides the final irradiance profile over the focal plane, and also over interior surfaces of the receiver, which is typically a cylindrical cavity.

These optical analysis computer programs are semi-automated, in that they not only predict the optical performance of the lens, but they also define the optimal configuration of each prism within the lens for the selected flux profile tailoring algorithm. For example, for the dome lens solar dynamic concentrator, for a given input value of the geometric concentration ratio (e.g., 800X), which is the lens aperture area divided by the receiver aperture area, the computer code can automatically configure each prism to direct the highest possible amount of focussed sunlight of all wavelengths coming from all parts of the solar disk into that receiver aperture. This is the algorithm used for the present study.

Figure 6-1 presents typical results from such an optical analysis. The tabulated results on the left correspond to the irradiance profile in the focal plane, which contains the cavity receiver aperture. The flux in suns is provided for each annular ring in the focal plane, with radial distances normalized by the dome lens aperture radius. For the design 800X geometric concentration ratio, the receiver aperture radius divided by lens aperture radius is 0.0354 (1/sqr[800]). Note that the net optical efficiency for this design receiver size is 86.7%, determined by integrating the energy incident over the receiver aperture. The same irradiance profile has also been integrated for a 0.25 degree tracking error, with the 84.5% result shown at the bottom of the figure. Note also that the peak irradiance at the center of the focal plane is 5,000 suns, relatively mild compared to some parabolic dish concentrators which have produced a spike of 15,000 suns (Reference 8).

The table on the right of Figure 6-1 shows the irradiance distribution within the cavity receiver, over the internal cylinder walls and over the internal flat back plate. These results assume a cylindrical cavity with an internal cylinder radius which is 7% of the lens aperture radius, and an internal length which is 20% of the lens aperture radius. These fractions are typical of cavity receivers (Reference 13). Note the very mild flux profile over the walls, with a peak of only 33 suns irradiance. Note also the relatively mild flux profile over the back plate, with a peak of 269 suns. Note also that 34% of the solar energy incident on the lens is deposited over the cylindrical walls, while 52.7% of the incident energy is deposited on the back plate, for the total of 86.7%, matching the focal plane value and the value presented in the previous section.

The results discussed above are for the final recommended lens design, which has a rim angle of 30 degrees, measured from the optical axis to the outermost prism in the lens. This near-optimal rim angle was determined through trade studies, which are summarized in Figure 6-2. The 30 degree rim angle provides the highest

ENTECH, INC.

Figure 6-1
NASA DOME LENS BRAYTON PROGRAM
OPTICAL ANALYSIS RESULTS
30 DEG. RIM ANGLE, 800X GCR

Dome Lens Optics Program

5 KWE NASA Brayton Dome Lens
Rim Angle (degrees) = 30
Integration step (degrees) = 5
Design Geometric Concentration Ratio (GCR) = 800
Design Tracking Error (deg) = 0
Receiver Cavity Radius/Lens Aperture Radius = .07
Receiver Cavity Length/Lens Aperture Radius = .2

| Annular Ring (Units of Aperture Radius) | | | Flux (Suns) | Cumulative Optical Efficiency (Percent) |
|---|---|---|---|---|
| 0 | - | 1.8e-03 | 4969 | 1.6 |
| 1.8e-03 | - | 3.5e-03 | 1718 | 3.2 |
| 3.5e-03 | - | 5.3e-03 | 3950 | 9.3 |
| 5.3e-03 | - | 7.1e-03 | 2928 | 15.7 |
| 7.1e-03 | - | 8.8e-03 | 2418 | 22.5 |
| 8.8e-03 | - | .0106 | 2145 | 29.9 |
| .0106 | - | .0124 | 1714 | 36.9 |
| .0124 | - | .0141 | 1188 | 42.4 |
| .0141 | - | .0159 | 1221 | 48.9 |
| .0159 | - | .0177 | 960 | 54.6 |
| .0177 | - | .0194 | 807 | 59.9 |
| .0194 | - | .0212 | 908 | 66.5 |
| .0212 | - | .023 | 477 | 70.2 |
| .023 | - | .0247 | 679 | 75.6 |
| .0247 | - | .0265 | 275 | 78.1 |
| .0265 | - | .0283 | 344 | 81.4 |
| .0283 | - | .0301 | 132 | 82.8 |
| .0301 | - | .0318 | 213 | 85.1 |
| .0318 | - | .0336 | 61 | 85.8 |
| .0336 | - | .0354 | 74 | 86.7 |
| .0354 | - | .0371 | 7 | 86.8 |
| .0371 | - | .0389 | 20 | 87.1 |
| .0389 | - | .0407 | 0 | 87.1 |
| .0407 | - | .0424 | 0 | 87.1 |
| .0424 | - | .0442 | 0 | 87.1 |
| .0442 | - | .046 | 11 | 87.3 |
| .046 | - | .0477 | 4 | 87.3 |
| .0477 | - | .0495 | 14 | 87.6 |
| .0495 | - | .0513 | 3 | 87.6 |
| .0513 | - | .053 | 23 | 88 |
| .053 | - | .0548 | 0 | 88 |
| .0548 | - | .0566 | 22 | 88.5 |
| .0566 | - | .0583 | 3 | 88.5 |
| .0583 | - | .0601 | 12 | 88.8 |
| .0601 | - | .0619 | 3 | 88.8 |
| .0619 | - | .0636 | 8 | 89 |
| .0636 | - | .0654 | 0 | 89 |
| .0654 | - | .0672 | 0 | 89 |
| .0672 | - | .0689 | 0 | 89 |
| .0689 | - | .0707 | 0 | 89 |

Aperture Radius/Focal Length = .462801426
Optical Efficiency with 0.25 deg Tracking Error = .844053164

| Internal Cavity Wall Location (Units of Aperture Radius) | | | Flux (Suns) | Cumulative Optical Efficiency (Percent) |
|---|---|---|---|---|
| 0 | - | .01 | 0 | 0 |
| .01 | - | .02 | 0 | 0 |
| .02 | - | .03 | 0 | 0 |
| .03 | - | .04 | 0 | 0 |
| .04 | - | .05 | 0 | 0 |
| .05 | - | .06 | 0 | 0 |
| .06 | - | .07 | 3 | .4 |
| .07 | - | .08 | 4 | 1 |
| .08 | - | .09 | 11 | 2.4 |
| .09 | - | .1 | 6 | 3.3 |
| .1 | - | .11 | 8 | 4.4 |
| .11 | - | .12 | 15 | 6.5 |
| .12 | - | .13 | 14 | 8.5 |
| .13 | - | .14 | 20 | 11.3 |
| .14 | - | .15 | 24 | 14.6 |
| .15 | - | .16 | 28 | 18.5 |
| .16 | - | .17 | 33 | 23.1 |
| .17 | - | .18 | 26 | 26.7 |
| .18 | - | .19 | 25 | 30.2 |
| .19 | - | .2 | 27 | 34 |

| Internal Cavity Back Location (Units of Aperture Radius) | | | Flux (Suns) | Cumulative Optical Efficiency (Percent) |
|---|---|---|---|---|
| 0 | - | 3.5e-03 | 0 | 0 |
| 3.5e-03 | - | 7e-03 | 13 | 0 |
| 7e-03 | - | .0105 | 38 | .3 |
| .0105 | - | .014 | 124 | 1.3 |
| .014 | - | .0175 | 217 | 3.7 |
| .0175 | - | .021 | 255 | 7.2 |
| .021 | - | .0245 | 269 | 11.5 |
| .0245 | - | .028 | 246 | 16 |
| .028 | - | .0315 | 211 | 20.4 |
| .0315 | - | .035 | 150 | 23.9 |
| .035 | - | .0385 | 114 | 26.8 |
| .0385 | - | .042 | 107 | 29.8 |
| .042 | - | .0455 | 101 | 32.9 |
| .0455 | - | .049 | 82 | 35.6 |
| .049 | - | .0525 | 62 | 37.9 |
| .0525 | - | .056 | 70 | 40.5 |
| .056 | - | .0595 | 67 | 43.2 |
| .0595 | - | .063 | 80 | 46.7 |
| .063 | - | .0665 | 58 | 49.3 |
| .0665 | - | .07 | 70 | 52.7 |

ORIGINAL PAGE IS
OF POOR QUALITY

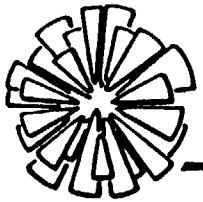

ENTECH, INC.

Figure 6-2
NASA DOME LENS BRAYTON PROGRAM
LENS RIM ANGLE OPTIMIZATION

| LENS RIM ANGLE (DEGREES) | NET OPTICAL EFFICIENCY @ 800X GCR WITH 0.00 DEG TRACKING ERROR | NET OPTICAL EFFICIENCY @ 800X GCR WITH 0.25 DEG TRACKING ERROR | |
|---|---|---|---|
| 15 | 86.2% | 78.4% | |
| 30 | 86.7% | 84.5% | *** OPTIMAL *** |
| 45 | 82.3% | 80.7% | |

optical efficiency for both perfect sun-pointing and for 0.25 degree sun-pointing error. A graphical depiction of the irradiance profile in the focal plane for this selected lens design is shown in Figure 6-3.

The selected 800X geometric concentration ratio was based on thermal analyses, which are discussed in the following section.

Figure 6-3

GRAPHICAL DEPICTION OF THE FOCAL PLANE RADIANT FLUX PROFILE FOR THE RECOMMENDED 30 DEG. RIM ANGLE LENS @ 800X GCR

(HIGHEST BAR REPRESENTS 4969 SUNS)

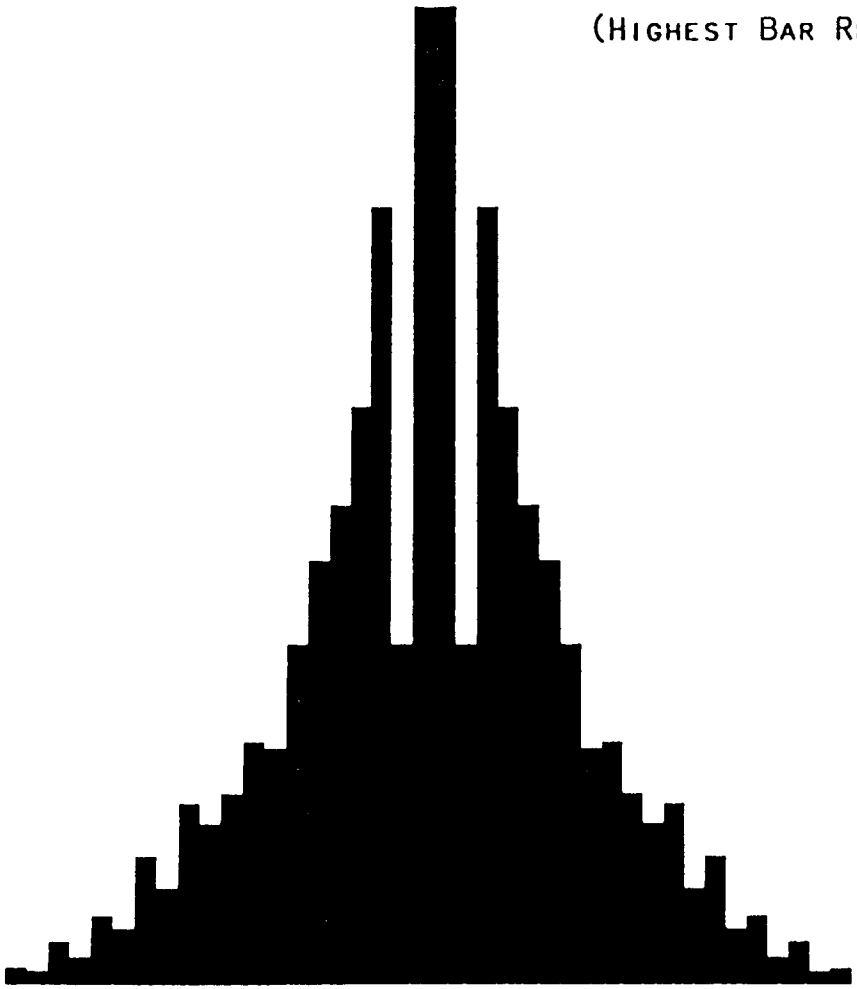

## 7.0 THERMAL ANALYSIS AND DISCUSSION

The selection of a recommended geometric concentration ratio (GCR) involves a trade-off of optical efficiency and receiver heat loss, which both decrease, but at different rates, with increasing GCR. Figure 7-1 summarizes this tradeoff for the dome Fresnel lens Brayton cycle solar dynamic system. The assumptions used in this trade-off are summarized in the upper portion of Figure 7-1. The receiver temperature and the radiation sink temperature were specified by NASA, as previously discussed in Section 4. The lens rim angle was selected based on optical considerations presented in Section 6. The lens material was assumed to be Kel-F 81, although the lens performance is relatively insensitive to material selection, provided that the optical properties (refractive index and absorption coefficient) in the solar spectrum are typical of glass and most transparent polymers. The receiver is assumed to be an efficient cavity, with an effective solar absorptance of 1.0 and an effective infrared emittance of 1.0 (i.e., a black body). No tracking error is included in the present calculation, although this effect was considered in Section 6.0.

The parametric results of the GCR trade-off study are presented in the lower portion of Figure 7-1. For each of the three GCR values considered, a new lens design was generated, with individual prism angles selected to provide the highest possible optical efficiency for the chosen GCR value. This prism angle optimization is accomplished by analytically evaluating the dispersed solar image produced by an individual prism, and by selecting the prism angle to place the infrared portion of the solar image near the closest edge of the receiver aperture, such that all or nearly all of the ultraviolet "tail" of the image falls within the opposite edge of the receiver aperture. By so selecting the prism angle, the highest possible receiver intercept factor is achieved, thereby maximizing overall optical efficiency. Note that the optical efficiency decreases slowly with increasing GCR. This decrease in optical efficiency is due to increasing ultraviolet spillage beyond the receiver aperture for smaller receiver aperture sizes. In contrast to this slow reduction in optical efficiency, the receiver heat loss decreases rapidly with increasing GCR, since the radiant heat loss is directly proportional to receiver aperture area. Note that the receiver heat loss corresponds to 8.3% of the solar irradiance incident on the dome lens aperture area for a GCR of 800X, and varies in inverse proportion to GCR for the other cases considered. The net thermal efficiency of the dome lens/receiver combination is simply the optical efficiency minus the receiver heat loss. Note that this thermal efficiency is the same for both 800X and 1000X, but is lower for 600X. The 800X GCR offers greater tolerances for deployment and tracking than the 1000X GCR, and is therefore the recommended value. Note that the calculated net thermal efficiency of the dome lens concentrator for this selected GCR is over 78%, an excellent value for such high-temperature solar heat collection.

The following section describes the conceptual design of the dome lens concentrator system.

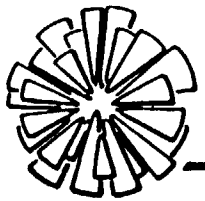

ENTECH, INC.

Figure 7-1

NASA DOME LENS BRAYTON PROGRAM
GEOMETRIC CONCENTRATION RATIO OPTIMIZATION

ASSUMPTIONS

* Brayton Receiver Temperature = 1121 K
* Radiation Sink Temperature = 225 K
* Direct Normal Insolation = 1353 w/sq.m.
* Dome Lens Rim Angle = 30 degrees (from Optic Axis)
* Dome Lens Material = Kel-F 81 (No Antireflection Coating)*
* Receiver Cavity Absorptance = 1
* Receiver Cavity Emittance = 1
* Tracking Error = 0 degrees

PARAMETRIC RESULTS

| GCR | NET OPTICAL EFFICIENCY | RECEIVER HEAT LOSS | NET THERMAL EFFICIENCY | |
|---|---|---|---|---|
| 600X | 87.3% | 11.0% | 76.3% | |
| 800X | 86.7% | 8.3% | 78.4% | *** Optimal *** |
| 1000X | 85.0% | 6.6% | 78.4% | |

CONCLUSION

Select 800X Instead of 1000X To Provide Greater Tolerances (Deployment & Tracking)

* KEL-F 81 WAS THE INITIAL MATERIAL ANALYZED. OPTICAL PERFORMANCE IS INSENSITIVE TO LENS MATERIAL SELECTION, PROVIDED THAT ABSORPTION IS NEGLIGIBLE AND DISPERSION IS COMPARABLE TO GLASS (conditions met by most transparent polymers).

## 8.0 CONCEPTUAL DESIGN AND DISCUSSION

The following paragraphs present the rationale and results of the conceptual design efforts related to the dome lens Brayton cycle power system, including considerations of configuration, size, deployment, structural integrity, and mass.

### 8.1 Lens Subdivisions to Facilitate Fabrication

Due to the relatively large size of the selected dome lens (i.e., 6.6 meters in aperture diameter), the lens must be subdivided into smaller, more manageable portions to facilitate fabrication of the lens. This subdivision involves three stages, as shown in Figure 8-1. Firstly, the dome is approximated with several different conical segments to eliminate compound curvature. Secondly, each conical segment is subdivided into a number of identical panels, which can be manufactured in flat form and then mechanically bent into the curved conical shape. Thirdly, each panel is subdivided into a number of identical, relatively small parquet elements, each of which consists of linear prisms which approximate the annular prisms of an ideal dome Fresnel lens. This third subdivision is necessary to allow practical tool-making, which involves the use of precise diamond turning equipment. By utilizing this three-stage subdivision approach, practical fabrication methods can be applied to the dome lens without adversely affecting its optical performance, provided that the conical segment annular extent (outer radius minus inner radius) is small compared to the lens aperture diameter and provided that the parquet element width is small compared to the receiver aperture diameter.

The panel subdivision approach is also convenient for compact stowage and automatic deployment, as discussed in the following sections.

### 8.2 Concentrator Configuration & Size

Figure 8-2 shows a side view of the selected 6.6 meter diameter dome lens concentrator system. The focal length of the lens along the optical axis is 7.2 meters. Thus, the F/D ratio of the 30-degree rim angle lens is 1.1. The lens/receiver support system consists of one main support beam and two tripod members. The receiver is integrated with the Brayton power conversion unit (PCU) and the waste heat radiator. As discussed in Section 3, the radiator can be oriented independently of the lens, since no lens aperture shading is ever caused by the radiator, in contrast to most reflective concentrator systems. Thus, the radiator can be maintained in an optimal orientation, such as one edge facing earth to minimize the interception of albedo and emitted radiation from the earth, and another edge facing forward to minimize residual atmospheric drag, which is a major concern in low earth orbit (LEO).

Figure 8-3 shows a front view of the dome lens concentrator. Nine different conical segments are used to approximate the ideal dome lens shape in the radial direction. Therefore nine different lens tools will be required to manufacture the lens. The dome lens is subdivided in the circumferential direction into twenty-four pie-shaped gores. Each gore comprises fourteen lens *panels*, corresponding to a single panel in each of the four inner conical segments, and two identical side-by-side panels in each of the five outer conical segments. Each lens panel is approximately 46 cm by 46 cm (18 inches by 18 inches), or smaller.

Figure 8-1

APPROXIMATIONS USED TO FABRICATE
DOME LENS CONCENTRATOR

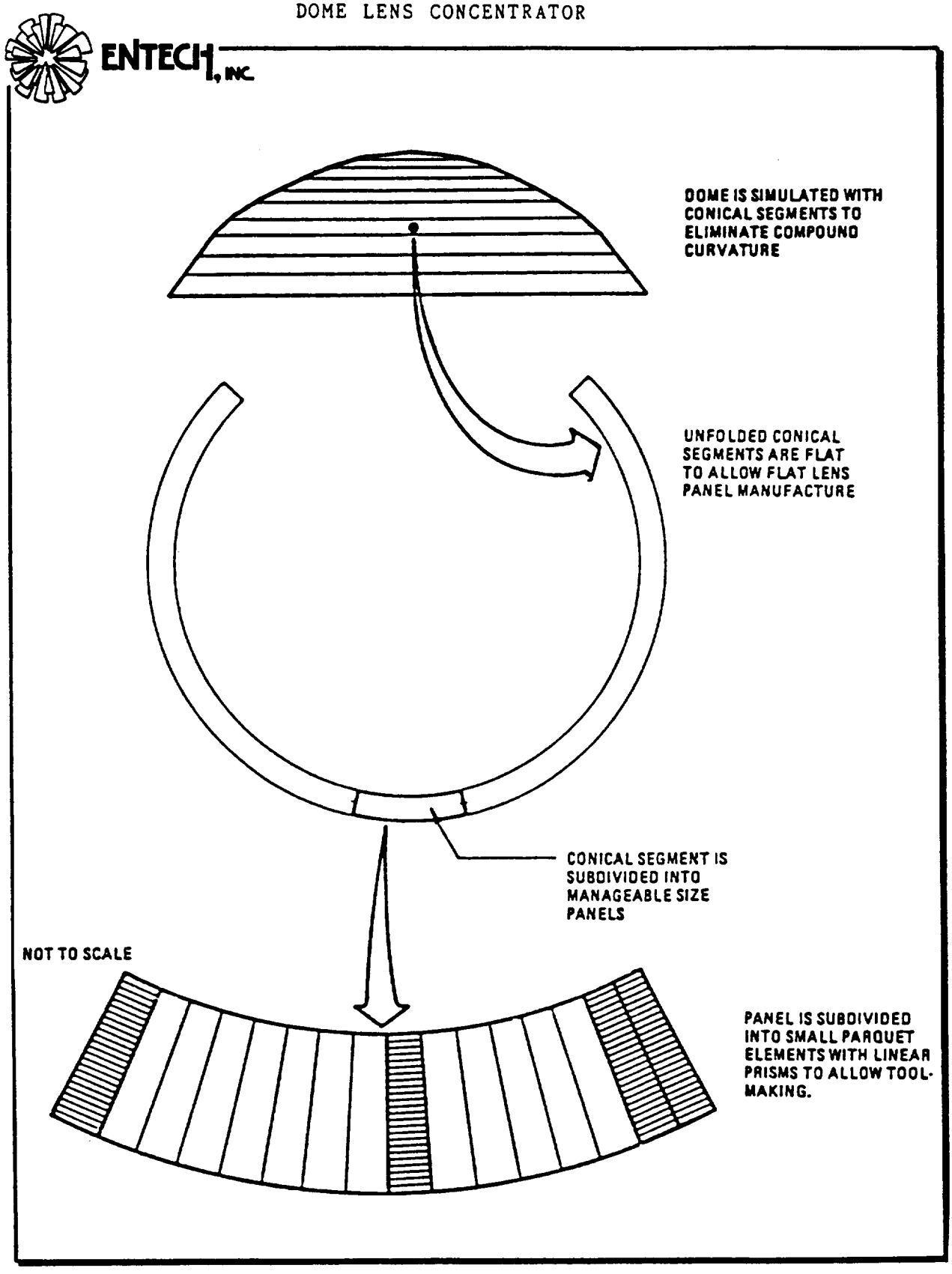

Figure 8-2

6.6 METER DIAMETER DOME LENS CONCENTRATOR
(SIDE VIEW)

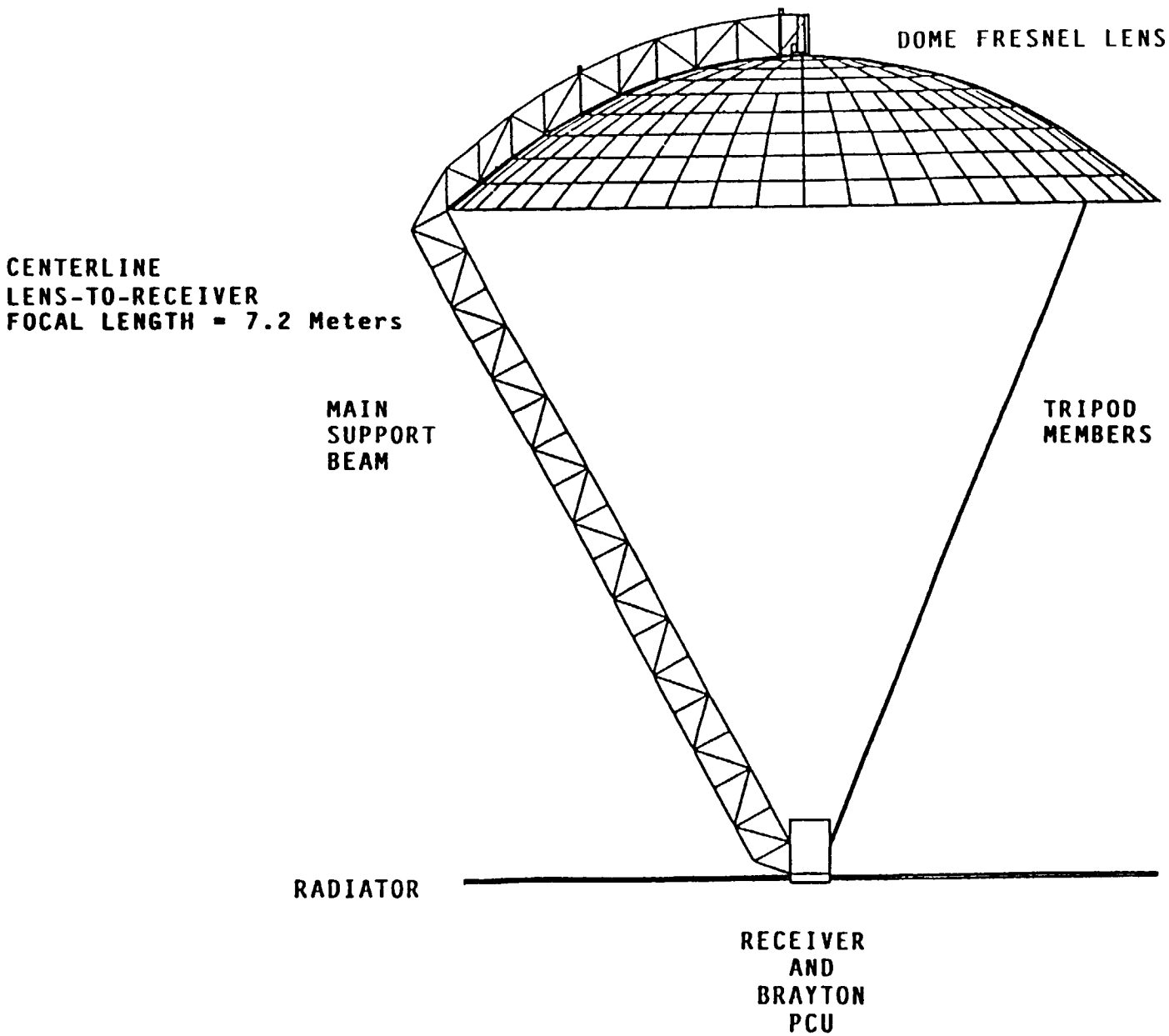

ENTECH, INC.

Figure 8-3

6.6 METER DIAMETER DOME LENS CONCENTRATOR
(FRONT VIEW)

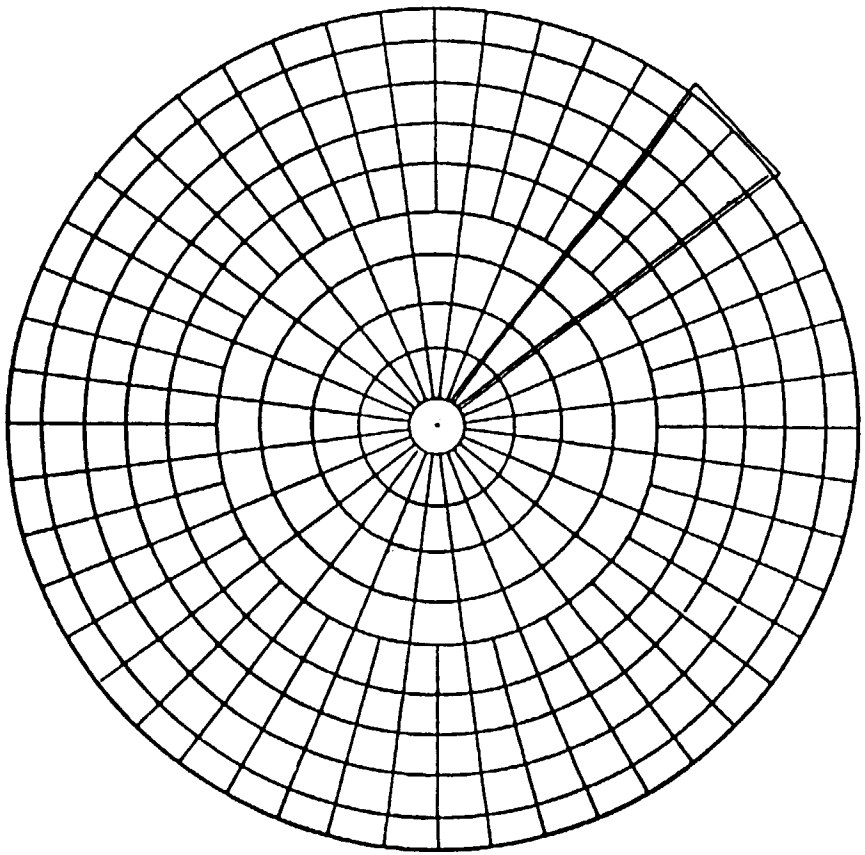

GEOMETRY: 24 GORES
14 LENS PANELS/GORE
9 DIFFERENT TOOLS
(EACH LENS TOOL
ABOUT 46 cm x 46 cm)

The gore approach to lens subdivision was selected to facilitate compact lens stowage and automatic deployment, as discussed in the following section.

## 8.3 Concentrator Stow & Deployment Approach

The selected approach to dome lens stowage and deployment is shown in Figures 8-4 and 8-5. The twenty-four gores are stowed by stacking them on top of one another to form a bundle contained within a space-frame truss structure. The volume of the stowed lens is approximately 0.6cubic meters, excluding the receiver, PCU, radiator, and lens/receiver connecting structure. For automatic deployment, the truss structure is held stationary, while the gores are incrementally deployed. Each gore is sequentially lowered from the bottom of the stack into its final axial position, latched to the center hub structure and to the adjacent gore (if any), and then rotated with all previously deployed gores by fifteen degrees about the optical axis. The full drop-latch-rotate deployment sequence is shown schematically in Figure 8-5. Electric motor drives will perform the drop, latch, and rotate functions. When all twenty-four gores have been deployed, the first gore will latch to the last gore, thereby completing the circle and forming an integrated dome lens concentrator.

After deployment of all twenty-four gores, the space-frame truss structure, which previously served as the gore container, now forms the rigid backbone of the dome lens concentrator. By interlocking, the gores also form a highly efficient lens support structure. The following section presents structural analyses of the dome lens concentrator.

## 8.4 Structural Analysis & Results

To evaluate the static and dynamic response of the dome lens, a finite element structural model was developed, as summarized in Figures 8-6, 8-7, and 8-8. Graphite/epoxy composite tubes, each 1.27 cm square in cross section with 0.043 cm walls, were selected to form the gore support structure. The lens panels were modeled as non-load-carrying plates, having an areal mass corresponding to 300 micrometer thick glass, with the plates supported by the gore tube matrix. The space-frame truss structure backbone of the dome lens was modeled as a set of fixed restraint nodes, while the rest of the lens was essentially cantilevered from this backbone.

The most severe loading condition envisioned for the deployed lens would correspond to terrestrial testing. Under this condition, loads could slightly exceed 1 G due to accelerations caused by sun tracking. This condition was therefore modeled as a 1.5 G load. Figures 8-9 and 8-10 present the deflections which the dome lens would experience due to 1.5 G loading in a direction parallel to the optical axis. Note that the graphical depictions of the lens deflections are highly exaggerated to make lens shape changes visible. In fact, the 13.7 cm maximum deflection is very small compared to the 6.6 meter aperture diameter of the lens. The stress levels in the most highly loaded tube are shown in Figure 8-11. In this tube, the bending stress is about 0.3 GN/sq.m. (40,000 psi), well below the 1.4 GN/sq.m. (200,000 psi) ultimate tensile strength of the material. These results indicate that the dome lens could be deployed and tested in the terrestrial environment prior to launch without damaging the structure. Such pre-flight testing under 1 G conditions could provide invaluable data regarding optical, thermal, mechanical, and structural performance.

Figure 8-4

LENS GORE STOWAGE PRIOR TO DEPLOYMENT
(CONCEPTUAL - NOT TO SCALE)

DRIVE FOR INCREMENTALLY ROTATING THE DEPLOYED GORES TO NEXT POSITION

DRIVES FOR INCREMENTALLY LOWERING THE GORE STACK AND LATCHING EACH GORE INTO ITS FINAL POSITION

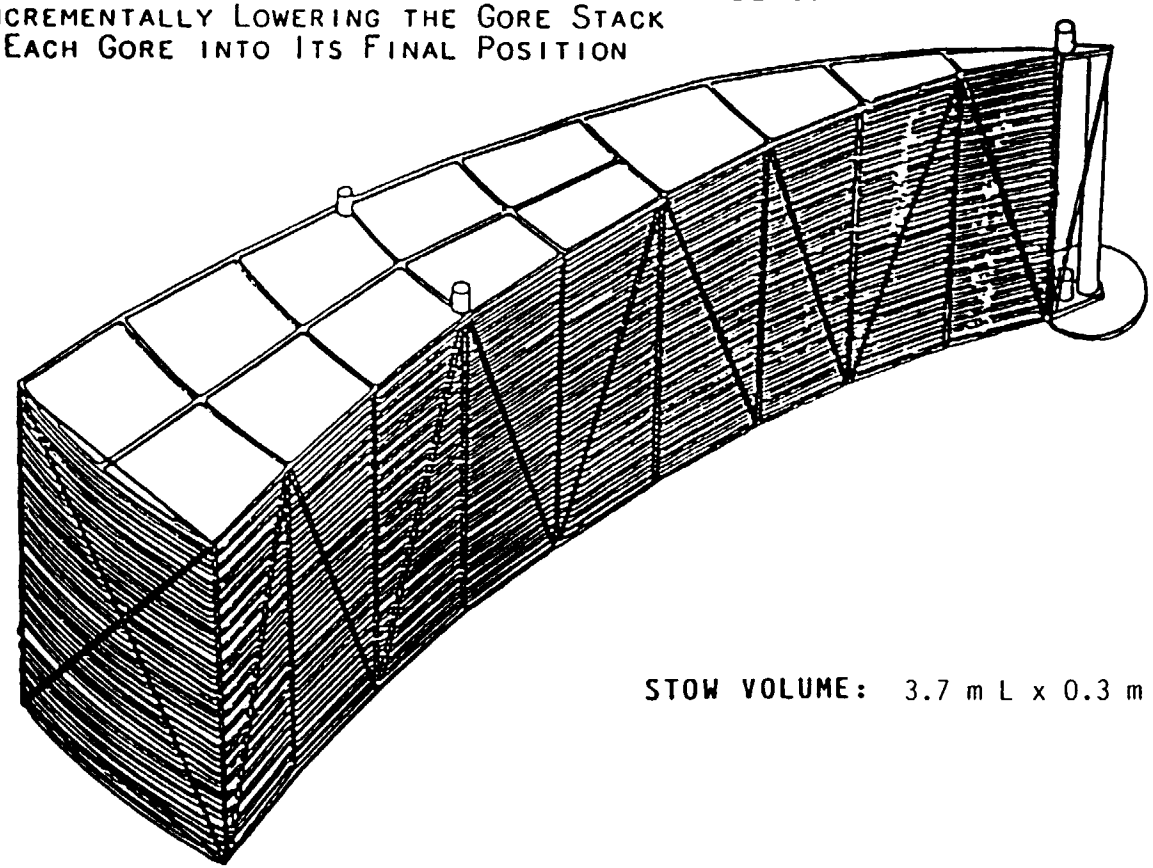

**STOW VOLUME:** 3.7 m L x 0.3 m D x 0.9 m Max W

Figure 8-5
DOME FRESNEL LENS DEPLOYMENT SEQUENCE

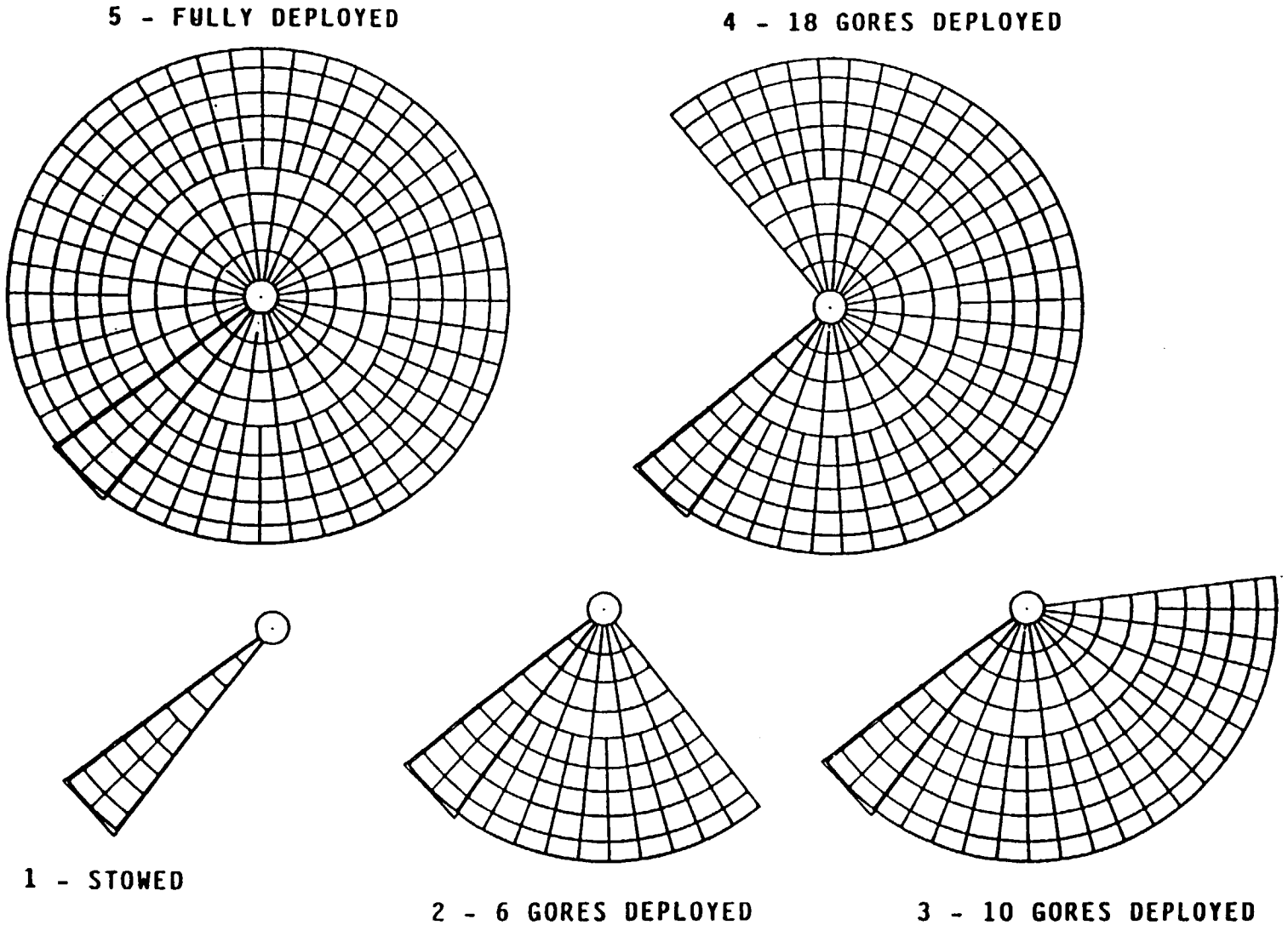

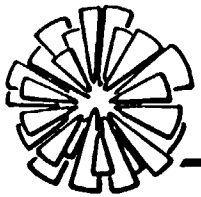


Figure 8-6

6.6 METER DIAMETER DOME FRESNEL LENS
CONCENTRATOR STRUCTURAL ANALYSIS

* THE DOME LENS CONCENTRATOR SUPPORT STRUCTURE WAS MODELED USING AN IBM-PC COMPATIBLE FINITE ELEMENT COMPUTER CODE (IMAGES 3D).

* STATIC AND DYNAMIC ANALYSES WERE CONDUCTED.

* THE MODEL INCLUDED 24 PIE-SHAPED GORE ASSEMBLIES.

* THE STRUCTURAL ELEMENTS WITHIN EACH GORE CONSISTED ENTIRELY OF 0.5 INCH SQUARE GRAPHITE/EPOXY TUBES, WITH THE FOLLOWING PROPERTIES:

| | |
|---|---|
| MODULUS OF ELASTICITY: | 55 GN/sq.m. |
| DENSITY: | 1384 kg/cu.m. |
| ULTIMATE TENSILE STRENGTH: | 1.4 GN/sq.m. |

* THE LENS ELEMENTS WERE ASSUMED TO BE MADE OF NON-LOAD-CARRYING 0.03 cm THICK GLASS, WHICH WAS ALLOWED TO "FLOAT" ON THE GRAPHITE/EPOXY TUBES.

ENTECH, INC.

Figure 8-7
DOME FRESNEL LENS CONCENTRATOR
STRUCTURAL MODEL - TOP VIEW

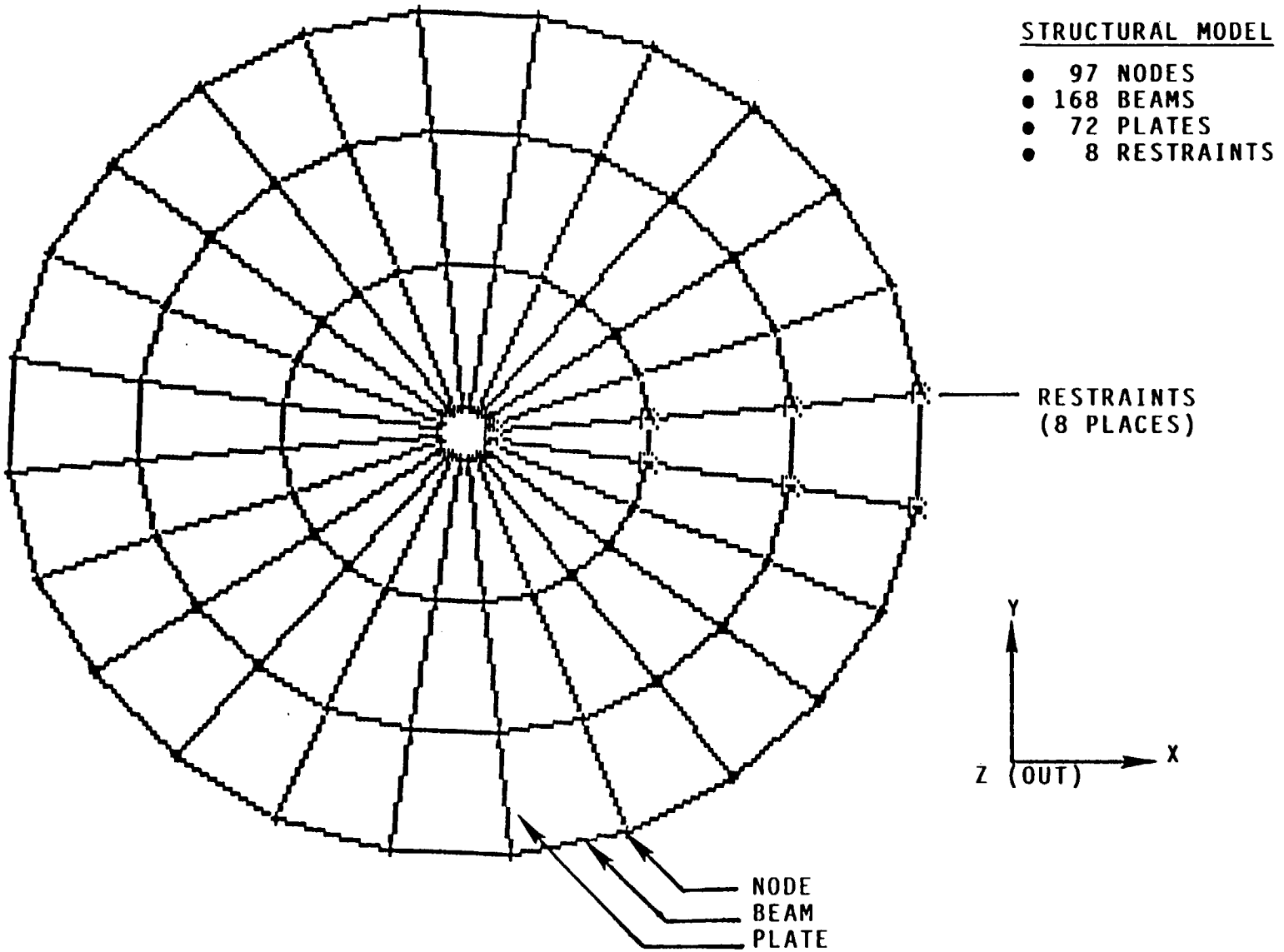

Figure 8-8

DOME FRESNEL LENS CONCENTRATOR
STRUCTURAL MODEL - SIDE VIEW

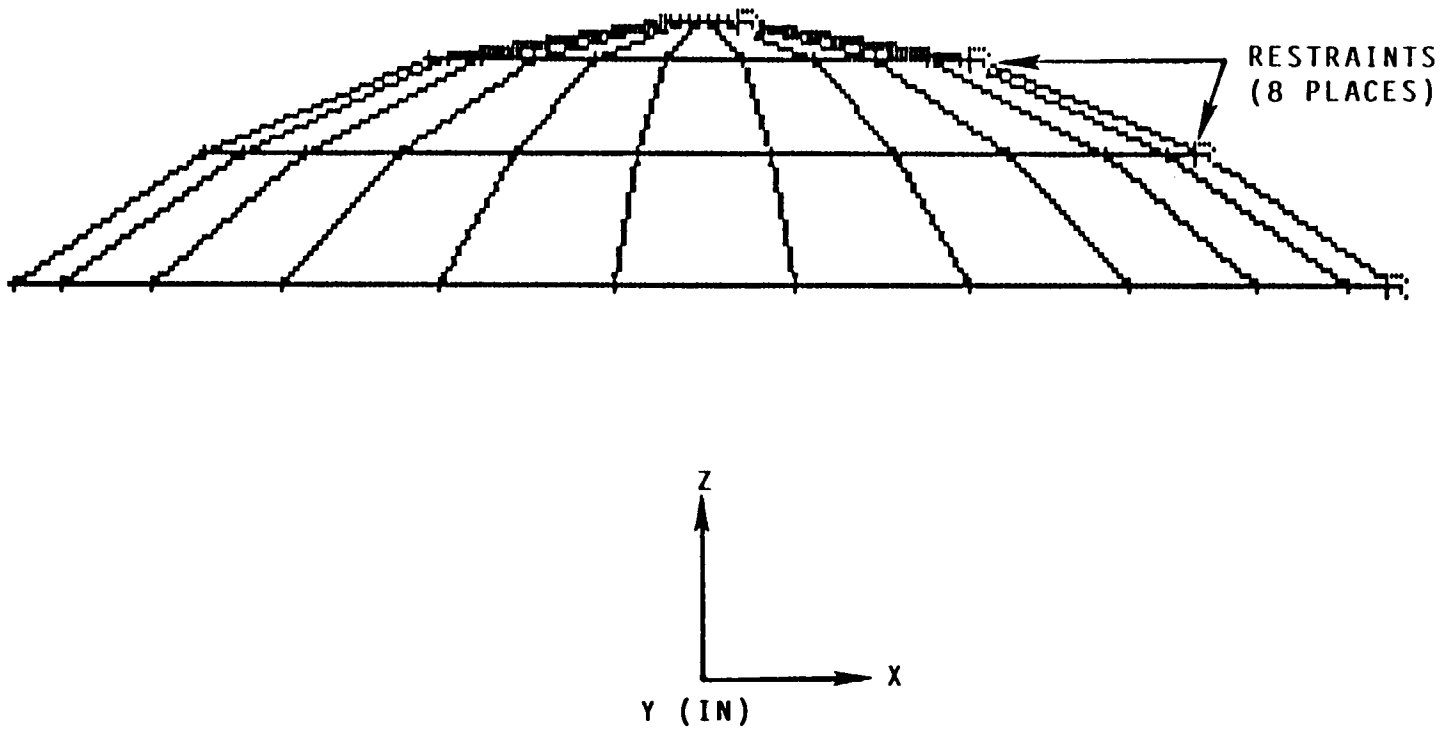

ENTECH, INC.

Figure 8-9
DOME FRESNEL LENS CONCENTRATOR
STRUCTURAL ANALYSIS RESULTS

DEFLECTED SHAPE UNDER 1.5-G LOADING (NEGATIVE Z-DIRECTION) (TOP VIEW)

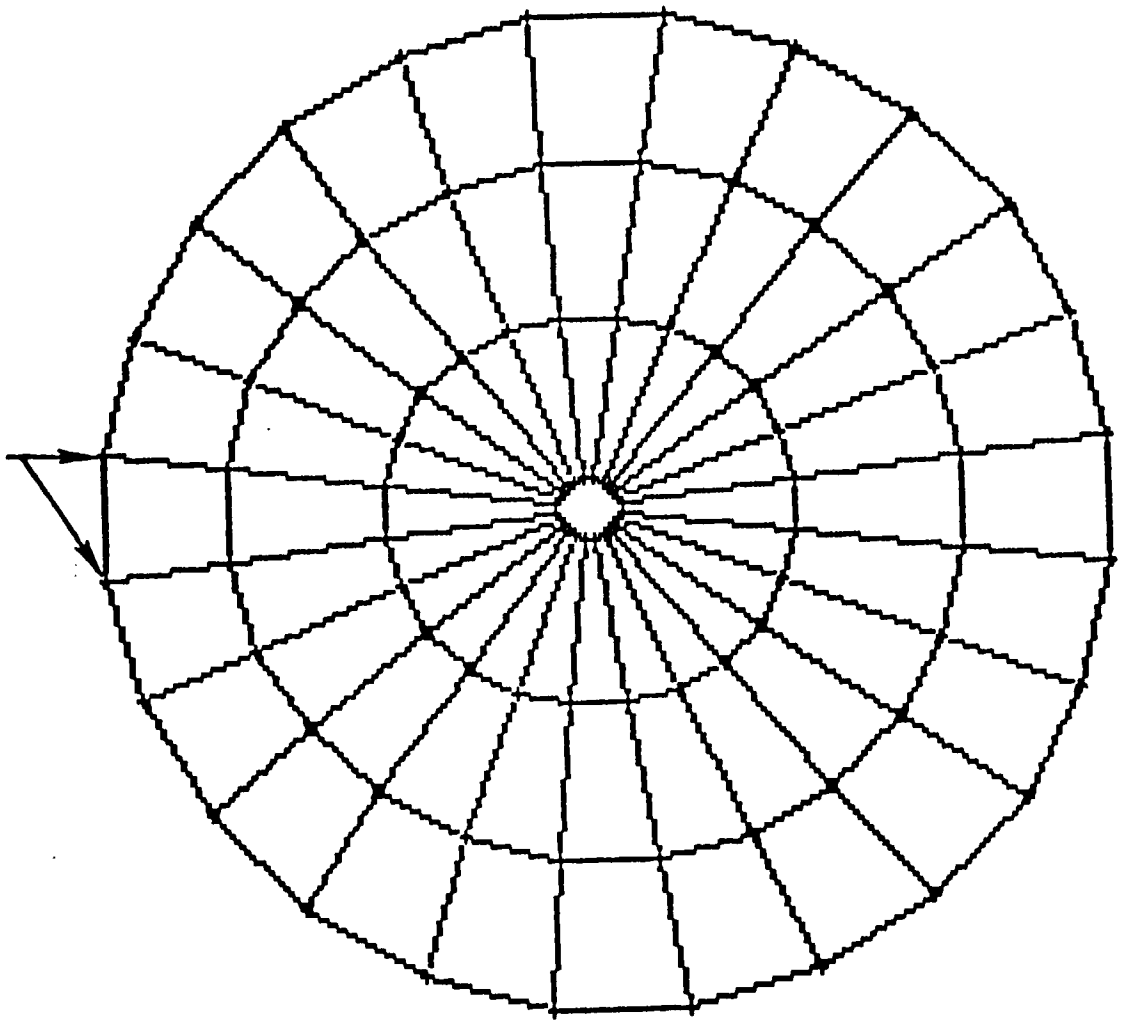


**MAX DEFLECTIONS**

$\Delta X$ = 4.7 cm
$\Delta Y$ = 0.6 cm
$\Delta Z$ = -13.7 cm

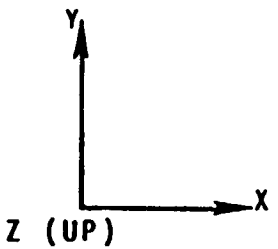

Figure 8-10

DOME FRESNEL LENS CONCENTRATOR
STRUCTURAL ANALYSIS RESULTS

DEFLECTED SHAPE UNDER 1.5-G LOADING (NEGATIVE Z-DIRECTION) (SIDE VIEW)

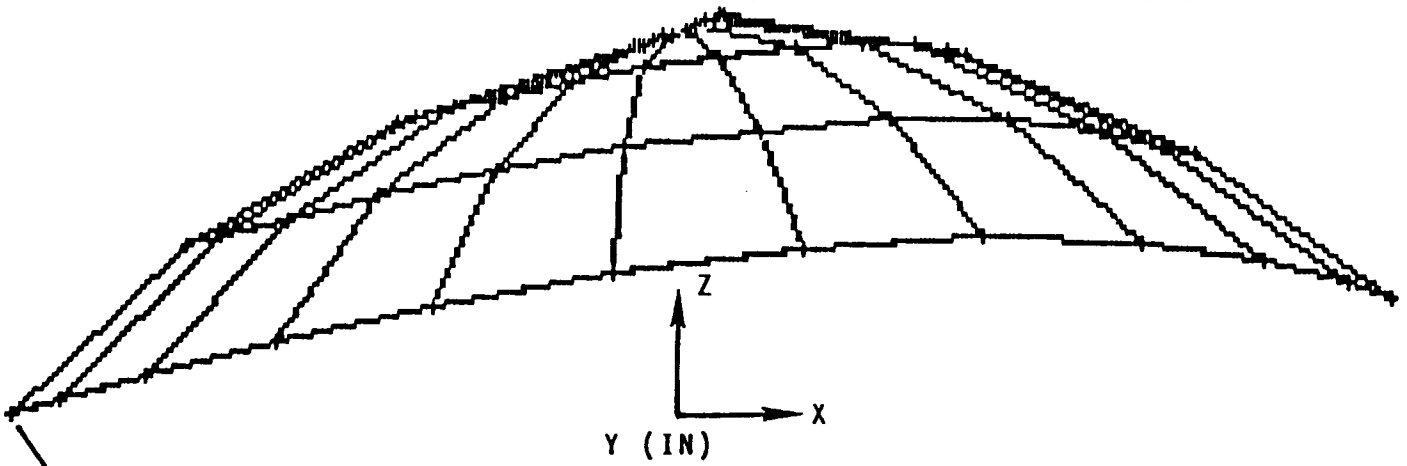


$\Delta X$ = 4.7 cm

$\Delta Y$ = 0.6 cm

$\Delta Z$ = -13.7 cm

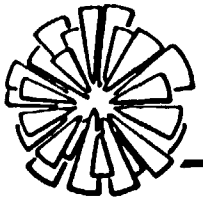

Figure 8-11

DOME FRESNEL LENS CONCENTRATOR
STRUCTURAL ANALYSIS RESULTS
MAX STRESS SUMMARY - BEAMS

ENTECH S/N:800777A 01-06-80
PAGE 1

========== I M A G E S 3 D ==========
= Copyright (c) 1984 Celestial Software Inc. =

SOLVE BEAM LOADS/STRESSES Version 1.3 03/01/86

**6.6 meter diameter dome fresnel lens structural analysis**

**Load Case 1:g-loading**

MAXIMUM STRESS* SUMMARY FOR BEAMS/TRUSSES
WITHIN SPECIFIED RANGE 1- 168

**Maximum (absolute) Stress =** 2.8 E + 08 **at BEAM** 96

| Beam | Axial | Y-Shear | Z-Shear | Torsion | Y-Bending | Z-Bending |
|---|---|---|---|---|---|---|
| 96 | 2.8 E+07 | 2.4E+06 | 2.7E+07 | 7.2E+07 | 9.3E+05 | 2.8E+08 |

*All stresses in N/sq.m.

The structural model was also used to analyze the dynamic behavior of the dome lens concentrator, with results shown in Figures 8-12, 8-13, and 8-14. The lowest natural frequency was found to be about one-half hertz, corresponding to a rotational oscillation about the structural backbone of the lens. This relatively high natural frequency is thought to be acceptable for most space missions.

The following section presents a mass estimate for the dome lens, including the lens panels and the tubular structure.

## 8.5 Concentrator Mass Estimate

The mass of the dome lens concentrator, excluding receiver, PCU, radiator, and lens/receiver interconnecting supports, is estimated in Figure 8-15. The lens panel mass is based on the most dense candidate lens material, glass, with an effective thickness of 300 micrometers (12 mils). The effective thickness is the sum of the base thickness plus one-half of the prismatic pattern thickness, since the prismatic pattern is half void (Refer back to Figure 3-2). The total mass of the glass would be 29 kg for the 6.6 meter diameter dome lens. The graphite/epoxy tubes, described in the previous section, have a cumulative mass of 8 kg. Adding a miscellaneous mass category, to include fasteners and the like, results in a total lens mass of 41 kg, or 1.21 kg per square meter of aperture. Most of the mass is in the lens panels, which could be made lighter either by using an alternate polymer material with a lower density than glass, or by decreasing the thickness of the glass. However, even the conservative 1.21 kg/sq.m. areal mass in Figure 8-15 is thought to be very competitive with alternate solar dynamic concentrator approaches, such as parabolic dishes.

The key technical challenge with the dome lens solar dynamic concentrator approach is associated with the lens material selection. The following section presents a summary of lens material evaluations conducted over the past several years.

Figure 8-12

DOME FRESNEL LENS CONCENTRATOR
DYNAMIC ANALYSIS RESULTS - TOP VIEW

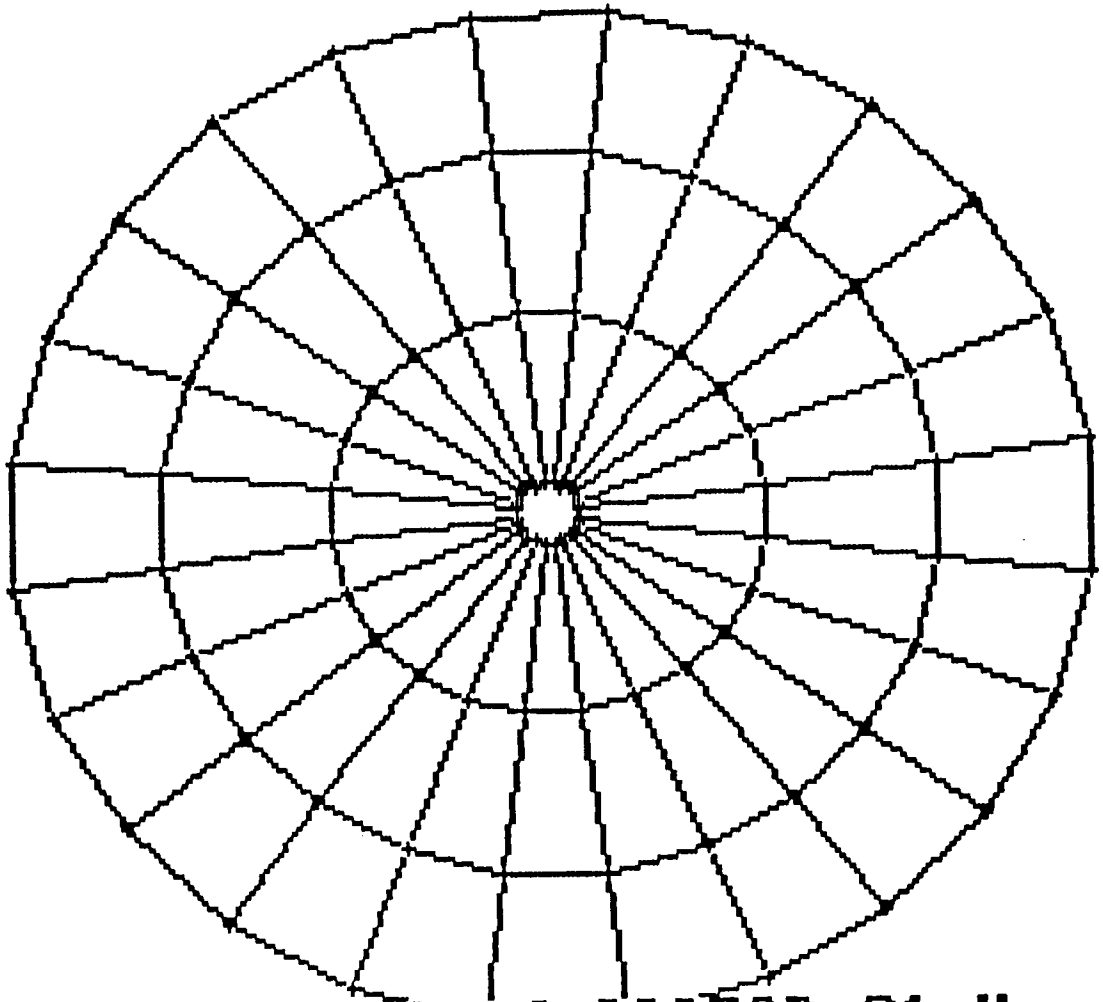

ENTECH, INC.

Figure 8-13
DOME FRESNEL LENS CONCENTRATOR
DYNAMIC ANALYSIS RESULTS - SIDE VIEW

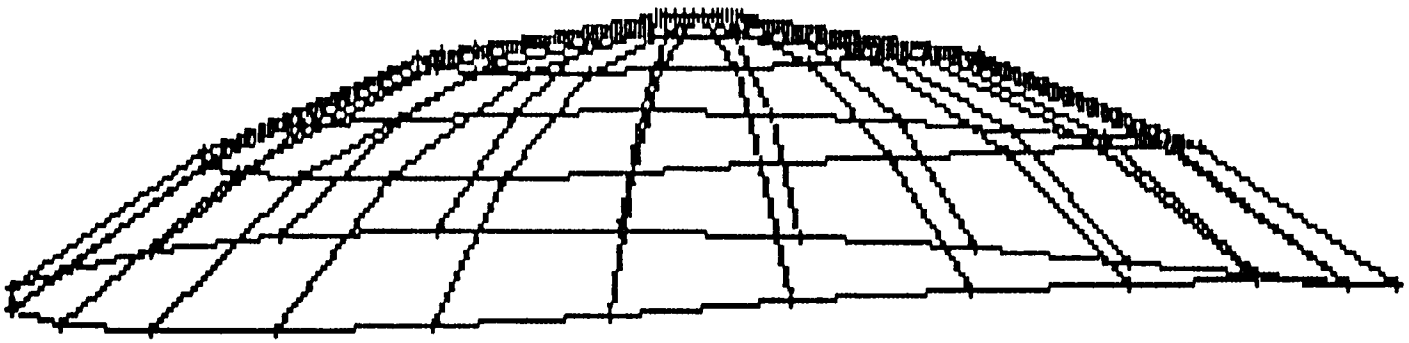

**Mode 1, 4.89979D-01 Hz.**

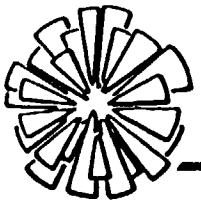

Figure 8-14
DOME FRESNEL LENS CONCENTRATOR
STRUCTURAL ANALYSIS RESULTS
DYNAMIC ANALYSIS

ENTECH S/N:800777A

01-06-80
PAGE 1

========== I M A G E S 3 D ==========
= Copyright (c) 1984 Celestial Software Inc. =
==========

SOLVE FREQUENCIES Version 1.3 03/01/86

**6.6 meter diameter dome fresnel lens structural analysis**

Number of frequencies requested 3
Number of frequencies printed 3
Acceleration of gravity 9.8 $m/sec^2$

| Mode | Eigenvalue | Frequency * | Period ** |
|---|---|---|---|
| 1 | .947794E+01 | .489979E+00 | .204091E+01 |
| 2 | .142656E+02 | .601129E+00 | .166354E+01 |
| 3 | .442585E+02 | .105881E+01 | .944455E+00 |

* Hertz
** Seconds

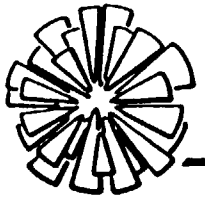

ENTECH, INC.

Figure 8-15

6.6 METER DIAMETER DOME FRESNEL LENS
CONCENTRATOR MASS ESTIMATE

| ELEMENT | MATERIAL | QUANTITY | MASS | MASS/APERTURE |
|---|---|---|---|---|
| LENS PANELS | GLASS | 39 sq. m. Surface<br>0.03 cm Eff. Thickness<br>2400 kg/cu.m. | 63 LB<br>29 KG | 0.17 LB/SQ.FT.<br>0.85 KG/SQ.M. |
| STRUCTURE | GRAPHITE/EPOXY | 268 Linear Meters<br>1.27 cm sq. Tube<br>0.043 cm Wall<br>1380 kg/cu.m | 18 LB<br>8 KG | 0.05 LB/SQ.FT.<br>0.24 KG/SQ.M. |
| MISC. | VARIOUS | 10% OF ABOVE | 8 LB<br>4 KG | 0.02 LB/SQ.FT.<br>0.12 KG/SQ.M. |
| TOTAL | | | 89 LB<br>41 KG | 0.24 LB/SQ.FT.<br>1.21 KG/SQ.M. |

## 9.0 LENS MATERIAL EVALUATION & DISCUSSION

In terrestrial solar concentrators using Fresnel lenses, acrylic plastic is the material of choice for the lens. This terrestrial lens material has nearly ideal properties, including high specular transmittance, low cost, ease of molding into prismatic patterns, excellent durability, and proven 25+ year lifetime in the terrestrial environment. Unfortunately, the more hostile space environment requires a different material with greater tolerance for high-energy ultraviolet radiation exposure and monatomic oxygen bombardment (in low earth orbit applications). Over the past several years, numerous materials have been evaluated for potential application in the dome Fresnel lens panels discussed in the previous section. These materials fall into two main categories: plastics and glass. If a transparent plastic could survive the hostile orbital environment, one would expect plastic to be superior to glass in terms of moldability, flexibility, low mass density, etc. Conversely, if glass could be molded into a prismatic shape, one would expect glass to be superior to plastic in terms of durability in the orbital environment. Until recently, no method of making all-glass prismatic lenses was available. Therefore, the leading lens material candidates were all moldable plastics, as further discussed in Section 9.1 below. Under the present program, a new sol-gel casting process was found to produce excellent prismatic shape replication in glass, as further discussed in Section 9.2 below. While none of the plastics has yet provided acceptable resistance to monatomic oxygen exposure, coatings are expected to eventually surmount the oxygen erosion problem. Likewise, while a substantial amount of process development remains to be done to establish the sol-gel process for manufacturing thin, relatively large lens panels, small-scale testing indicates that such a process will eventually be feasible.

### 9.1 Moldable Plastics

A wide variety of moldable, transparent plastic materials have been supplied to NASA Lewis for monatomic oxygen exposure testing in a plasma asher facility. These materials include various acrylics, polycarbonates, silicones, fluoropolymers, and polyimides. For every sample, after oxygen fluences corresponding to less than ten years of low earth orbit (LEO) operation, the exposed surface was severely eroded, thereby substantially lowering the specular transmittance. To overcome this surface erosion problem, a number of thin coatings have been applied to the various lens sample materials. These coatings have included magnesium fluoride, silicon oxide, sol-gels, and similar thin film coatings. To date, either the coating application immediately reduced the specular transmittance of the sample to unacceptable levels, or the coating failed to inhibit the oxygen erosion.

The only moldable plastic lens materials tested to date which have survived monatomic oxygen exposure without degradation have been those protected by a layer of glass. Sample composites of silicone rubber with a protective microglass superstrate suffered no degradation in the asher testing. This composite lens approach is currently being utilized for photovoltaic concentrator applications (References 14, 15, and 16). However, even in small thicknesses, glass is relatively heavy due to its high density (more than double the density of most plastics). Therefore, a thin-film protective coating is still highly desirable for space Fresnel lens applications.

In summary, no moldable plastic material has yet been identified which is capable

of surviving monatomic oxygen exposure without a protective glass superstrate. If such a glass superstrate is required to protect the plastic, why not make the whole lens out of glass and forget the plastic? Until recently, no method existed for making high-quality Fresnel lenses from glass. However, under the present program, proof-of-concept glass Fresnel lens samples have been successfully made by a new sol-gel casting process, as discussed in the following section.

## 9.2 Densified Sol-Gel Glass

During the course of the present program, a potential new process for making all-glass Fresnel lenses was identified. The new glass fabrication process if being developed for other glass products by Gel-Tech, Inc., of Alachua, Florida. The process involves the low-temperature casting, followed by stabilization and high-temperature densification, of a sol-gel material, resulting in a high-quality silica glass product. Following a visit to Gel-Tech by NASA and ENTECH personnel, a contract modification was implemented to allow a proof-of-concept experiment to be conducted. In the past, all of Gel-Tech's optical products had utilized monolithic glass geometries (e.g., convex lenses and solid cylinders). Under this present program, using tooling to be supplied by ENTECH, Gel-Tech was to attempt for the first time to accurately replicate a prismatic lens geometry in the densified sol-gel material. The key technical issue related to such prismatic lens replication involves the drastic shrinkage produced during the stabilization and densification stages of the process. Compared to the tool, the final part exhibits about a 50% shrinkage in each of its three dimensions (i.e., casting a 2 cm cube results in a 1 cm cube). The goal of the experiment was to determine whether or not the triangular prisms in a Fresnel lens would maintain their shape, and merely be reduced in scale, during stabilization and densification. Fortunately, as discussed in the following paragraphs, the experiment demonstrated that excellent geometric replication, with a simple reduction in prism scale, was possible with the sol-gel process.

To facilitate sample evaluation, a simple rectilinear prismatic pattern was selected for the experiment. This pattern consisted of side-by-side isosceles triangular prisms, each having a 90 degree apex angle. The starting size of the prisms corresponded to a lateral separation of 0.1 cm (0.04 inch). Since diamond-cut master tooling is generally metallic, and since the sol-gel liquid is highly corrosive to metal, plastic replica tooling had to be utilized as the sol-gel mold material. The first few candidate plastics, including acrylic, epoxy, and silicone rubber, were all attacked by the sol-gel liquid. Finally, polystyrene tooling was tried and it was found to be stable in contact with the sol-gel liquid. Several polystyrene tools, each 5 cm (2 inches) square, were then provided to Gel-Tech for proof-of-concept molding of sol-gel parts.

Since the key issue to be addressed in the proof-of-concept experiments was prismatic replication, it was decided to produce relatively thick samples (e.g., 0.3 cm) consistent with current Gel-Tech products, rather than trying to produce the ultimate thin lenses needed for space applications.

Two types of sample lenses were produced by Gel-Tech and delivered to ENTECH. One type was stabilized and fully densified, while the other was only stabilized and not fully densified. Figure 9-1 shows two photomicrographs of a white silicone impression of a fully densified sample. Note the excellent replication of the prismatic pattern, including prism angles, tip and valley sharpness, and

Figure 9-1

SOL-GEL LENS SAMPLES - PHOTOMICROGRAPHS
OF SILICONE IMPRESSIONS OF PRISMS
(BLACK REPRESENTS SOL GEL)

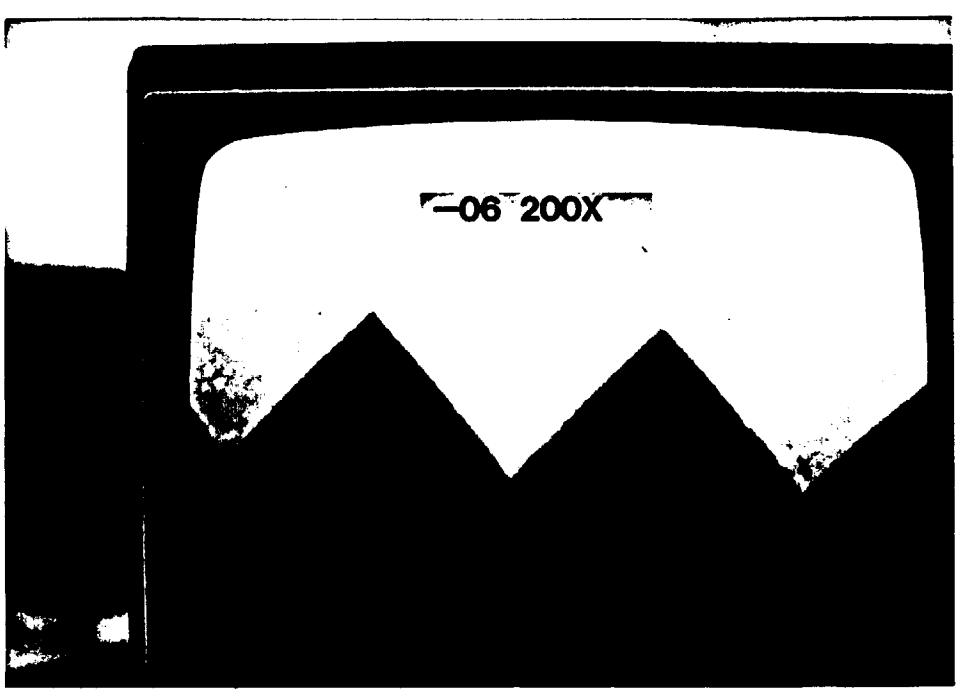


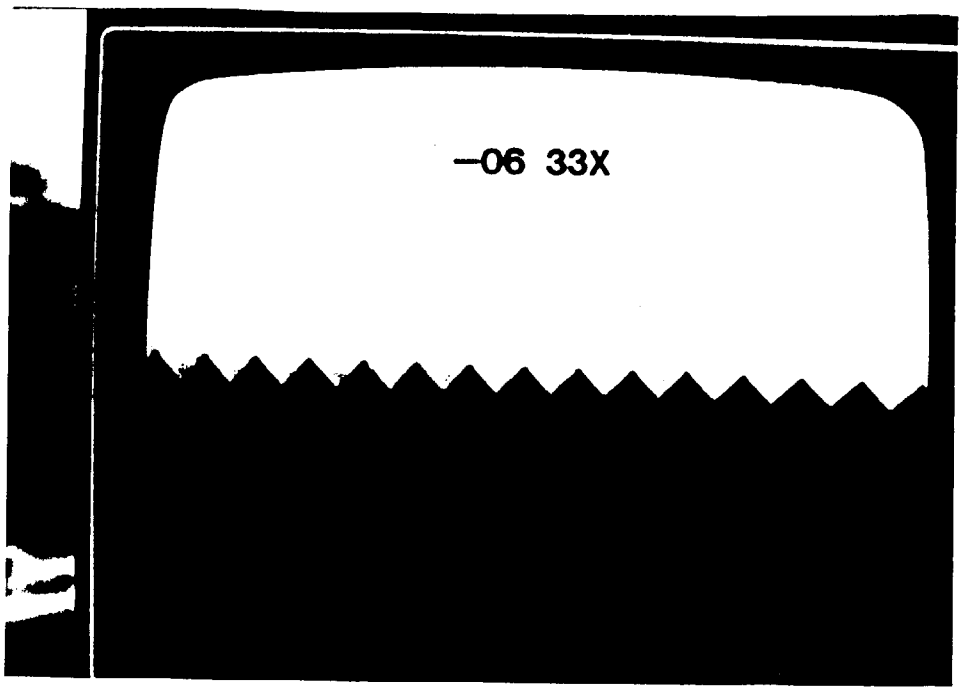

prism-to-prism spacing. Figure 9-2 shows similar photomicrographs of a stabilized (not densified) sample. This sample likewise shows excellent replication accuracy. The dimensions of the samples uniformly showed slightly over a 50% shrinkage. The final parts were slightly under 2.5 cm (1 inch) square and the prismatic spacing was slightly under 0.05 cm (0.02 inch). Despite this large shrinkage, the each prism retained a shape which was geometrically similar (i.e., identical except for scale) to the shape on the starting tool. Tests were conducted to verify the angular accuracy and the optical clarity of the samples, as discussed below.

Using a helium neon laser as the light source, a ray was passed through the fully densified sample, entering the smooth surface and exiting the prismatic surface. The sample was rotated until the minimum ray deviation angle was found, and this angle was measured. Using refractive index data supplied by Gel-Tech, the prism angle was calculated based on the measured minimum ray deviation angle. This deduced prism angle matched the 45 degree starting angle well within the accuracy of the deviation angle measurement.

Using the same laser light source, another test was run with the fully densified sample. The laser beam was passed through the sample, this time perpendicularly entering the prismatic side and exiting the smooth side as two distinct beams (due to the prismatic refraction). The two beams were collected by a silicon solar cell. The ratio of the solar cell's short-circuit current output with the sample in place to its current output without the sample in place provides a direct measurement of the transmittance of the sample. These measurements indicated a sample transmittance of approximately 90%, as anticipated based on Gel-Tech spectral transmittance data for smooth-surface samples of the densified sol-gel glass.

The samples were then delivered to NASA Lewis for further evaluation.

In summary, the new sol-gel process appears to be a technically feasible way of producing all-glass Fresnel lenses. However, much development remains to be done to scale up the process to produce larger area panels, and to minimize the thickness of the lenses. However, the prismatic replication question was considered to be the most difficult hurdle for the new process, and this question appears to have been successfully answered by the tests discussed above.

Figure 9-2

SOL-GEL LENS SAMPLES - PHOTOMICROGRAPHS
OF SILICONE IMPRESSIONS OF PRISMS
(BLACK REPRESENTS SOL GEL)

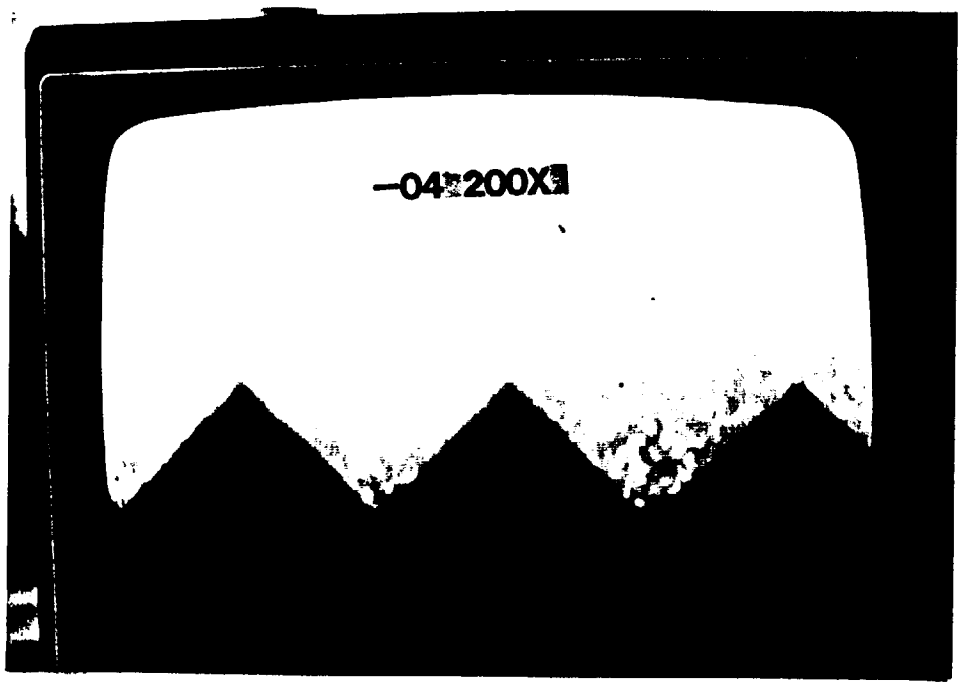


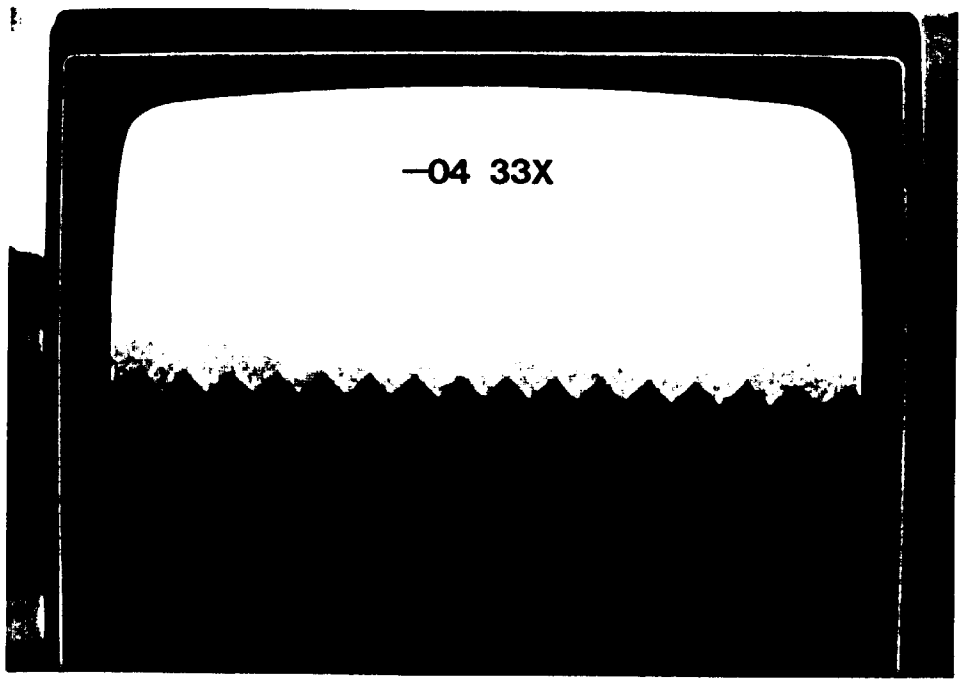

## 10.0 CONCLUSIONS

The key conclusions drawn from this conceptual design study are summarized below.

1. The dome Fresnel lens Brayton cycle solar dynamic concentrator approach should provide excellent optical, thermal, and electrical performance in orbital applications.

2. For 5 kW of continuous electrical output in low earth orbit, the dome lens optical concentrator will be about 6.6 meters in diameter and will have a mass of approximately 40 kg, if the lens panels are made of relatively heavy microglass.

3. The lens provides substantial advantages over more conventional solar dynamic concentrator approaches (e.g., parabolic dish reflectors), including 200 times larger slope error tolerance, zero aperture blockage by the power conditioning unit (including receiver and radiator), a milder (safer) focal plane irradiance profile, and the flexibility to tailor the irradiance profile over receiver heat exchanger surfaces by proper selection of prism angles.

4. The selected lens configuration includes a 7.2 meter focal length, a 30 degree rim angle, and a 0.25 degree tracking error budget. Expected lens performance is characterized by 87% net optical efficiency at 800X geometric concentration ratio.

5. Coupled with a cavity heat receiver operating at 1121 K, the overall thermal efficiency of the dome lens concentrator is expected to be an excellent 78%.

6. For ease of fabrication, compact stowage, and automatic deployment, the dome lens is configured in a 24-gore geometry. Deployment occurs in a drop, latch, rotate sequence, which utilizes the gore launch container as the structural backbone of the deployed lens.

7. Structural analyses indicate that the dome lens can be tested in a fully deployed condition under terrestrial gravity without damage to the graphite/epoxy tubular gore supports. The ability to tolerate such pre-flight tests is thought to be another major advantage of the dome lens approach.

8. The lens material issue remains the biggest hurdle to early space application of the dome lens concept.

9. None of the candidate moldable plastic lens materials has yet passed the monatomic oxygen exposure tests at NASA Lewis. Coatings need to be developed to protect these materials from surface erosion by the oxygen atoms.

10. Densified sol-gel all-glass Fresnel lens samples were successfully made and tested under this program. With further development, this new sol-gel process should be capable of providing high-quality, large-area, thin Fresnel lens panels for use in the dome Fresnel lens solar concentrator.

## 11.0 REFERENCES


1. "Sunflower Solar Collector," Accession No. N64-20889, NASA CR-46, May 1964.

2. E.F. Binz and J. Hartung, "Solar Dynamic Power for Space Station IOC," 21st IECEC, San Diego, August 1986.

3. "Solar Concentrator Advanced Development," Phase I Final Report, NASA Contract No. NAS3-24666, Harris Corporation, 1986.

4. M.J. O'Neill, "Dome Fresnel Lens Concentrator for Space Solar Dynamic Power," 21st IECEC, San Diego, August 1986.

5. D.L. Nored and D.T. Bernatowicz, "Electrical Power System Design for the U.S. Space Station," 21st IECEC, San Diego, August 1986.

6. J.E. White et al, "Optimization of Spherical Facets for Parabolic Solar Concentrators," 21st IECEC, San Diego, August 1986.

7. E.W. Dennison and T.O. Thostesen, "Development and Testing of Parabolic Dish Concentrator No. 1," JPL Publication 85-4, Pasadena, December 1984.

8. M.J. O'Neill and S.L. Hudson, "Optical Analysis of Paraboloidal Solar Concentrators," Annual Meeting of American Section of ISES, Denver, August 1978.

9. P.L. Panda et al, "Summary Assessment of Solar Thermal Parabolic Dish Technology for Electrical Power Generation," JPL Publication 85-55, Pasadena, September 1985.

10. M.J. O'Neill, "Solar Concentrator and Energy Collection System," U.S. Patent No. 4,069,812, January 1978.

11. M.J. O'Neill, "A Unique New Fresnel Lens Solar Concentrator," Silver Jubilee Congress of ISES, Atlanta, May 1979.

12. M.J. O'Neill and R.A. Waller, "Analytical/Experimental Study of the Optical Performance of a Transmittance-Optimized Linear Fresnel Lens Solar Concentrator," Annual Meeting of ISES, Phoenix, June 1980.

13. M.J. O'Neill, "A Dome Fresnel Lens Concentrator for the Space Station Solar Dynamic Power System," Final Report to Harris Corporation under Subcontract No. 5074148, ENTECH, Inc., DFW Airport, Texas, April 1986.

14. M.J. O'Neill et al, "The Mini-Dome Lens Space Concentrator Array: Recent Component Test Results and Current Array Development Status," 24th IECEC, Washington, August 1989.

15. M.F. Piszczor and M.J. O'Neill, "Development of an Advanced Photovoltaic Concentrator System for Space Application," NASA TM 100101, Cleveland, August 1987.

16. M.F. Piszczor and M.J. O'Neill, "Domed Fresnel Lens Concentrator Technology for Space Application," 9th NASA SPRAT Conference, Cleveland, April 1988.

NASA

# Report Documentation Page

| 1. Report No. | 2. Government Accession No. | 3. Recipient's Catalog No. |
|---|---|---|
| NASA-CR-185134 | | |

**4. Title and Subtitle**
Conceptual Design Study of a 5 Kilowatt Solar Dynamic Brayton Power System Using a Dome Fresnel Lens Solar Concentrator

**5. Report Date**
December 1989

**6. Performing Organization Code**

**7. Author(s)**
Mark J. O'Neill
A. J. McDanal
Don H. Spears

**8. Performing Organization Report No.**
None

**10. Work Unit No.**
506-41-31

**9. Performing Organization Name and Address**
ENTECH, Inc.
P. O. Box 612246 (1015 Royal Lane)
Dallas-Fort Worth Airport, TX 75261

**11. Contract or Grant No.**
NAS3-24877

**13. Type of Report and Period Covered**
Contractor Report
Final

**12. Sponsoring Agency Name and Address**
National Aeronautics & Space Administration
Lewis Research Center
Cleveland, OH 44135-3191

**14. Sponsoring Agency Code**

**15. Supplementary Notes**
Project Manager, Miles O. Dustin, Power Technology Division, NASA - Lewis Research Center

**16. Abstract**

The primary project objective was to generate a conceptual design for a nominal 5 kW solar dynamic space power system, which uses a unique, patented, transmittance-optimized, dome-shaped, point-focus Fresnel lens as the optical concentrator. Compared to reflective concentrators, the dome lens allows 200 times larger slope errors for the same image displacement. Additionally, the dome lens allows the energy receiver, the power conversion unit (PCU), and the heat rejection radiator to be independently optimized in configuration and orientation, since none of these elements causes any aperture blockage. Based on optical and thermal trade studies, a 6.6 m diameter lens with a focal length of 7.2 m was selected. This lens should provide 87% net optical efficiency at 800X geometric concentration ratio. The large lens is comprised of 24 gores, which compactly stow together during launch, and automatically deploy on orbit. The total mass of the microglass lens panels, the graphite/epoxy support structure, and miscellaneous hardware is about 1.2 kg per square meter of aperture. The key problem for the dome lens approach relates to the selection of a space-durable lens material. Under this project, for the first time, all-glass Fresnel lens samples were successfully made by a "sol-gel" casting process.

| 17. Key Words (Suggested by Author(s)) | 18. Distribution Statement |
|---|---|
| Fresnel Lens<br>Solar Dynamic<br>Solar Concentrator | Unclassified - Unlimited<br>Subject Category - 20 |

| 19. Security Classif. (of this report) | 20. Security Classif. (of this page) | 21. No of pages | 22. Price* |
|---|---|---|---|
| Unclassified | Unclassified | 47 | A03 |

NASA FORM 1626 OCT 86

*For sale by the National Technical Information Service, Springfield, Virginia 22161